arXiv:q-bio/0409027v2 [q-bio.GN] 28 Sep 2004

Characterizing large scale base composition structures of genomes

Zhengqing Ouyang[1], Jian Liu[1] and Zhen-Su She[1,2,*]
[1] *State Key Lab for Turbulence and Complex Systems and Center for Theoretical Biology, Peking University, Beijing 100871, P.R. China*
[2] *Department of Mathematics, UCLA, Los Angeles, CA 90095, USA*
(Dated: February 9, 2008)

Intermittent density fluctuations of nucleotide molecules (adenine, guanine, cytosine and thymine) along DNA sequences are studied in the framework of a hierarchical structure (HS) model originally proposed for the study of fully developed turbulence [She and Lévêque, Phys. Rev. Lett. **72**, 336 (1994)]. Large scale ($10^3 \leq \ell \leq 10^5$ bp) base density fluctuation is shown to satisfy the HS similarity. The derived values of a HS parameter β from a large number of genome data (including Bacteria, Archaea, human chromosomes and viruses) characterize different biological properties such as strand symmetry, phylogenetic relations and horizontal gene transfer. It is suggested that the HS analysis offers a useful quantitative description for heterogeneity, sequence complexity and large scale structures of genomes.

PACS numbers: 87.14.Gg; 87.15.Aa; 87.15.Cc

I. INTRODUCTION

The DNA sequence of a complete genome of an organism contains the information not only for making all the proteins (genes) necessary for the organism, but also for assembling them to form the organism in a specific time order with specific three-dimensional patterns. While small-scale (from several to hundreds base pairs) patterns of the nucleotide arrangement are certainly important for determining its coding or non-coding nature and some regulatory biological functions (e.g. binding site or splicing site signal) [1], more large-scale variation across several thousands base pairs or longer may be related to higher level biological functions such as controlling networks of genes which are likely important indices in evolution [2]. It is important to develop tools for analyzing these patterns with the available sequence data and to use it as a laboratory for quantitative exploring biological laws such as the mechanism of biological evolution [3].

There has been considerable efforts in studying the statistical property of nucleotide distribution pattern [4]. The concept of "domains-within-domains" has been introduced in Ref. [5] and confirmed in Ref. [6]. The algorithms for DNA sequence alignment and similarity search have been developed for the study of phylogeny and evolution of many biological species [7]. Other methods developed in nonlinear analysis and information theory were introduced to characterize coding and non-coding DNA sequences [8]. Beside these studies focused on local motifs of the DNA sequence, many other methods, including statistical physics analysis [9], spectrum analysis [5, 10, 11], wavelet analysis [12], etc, have also been proposed to measure the correlation between nucleotides over long distances along one-dimensional DNA chain. Although long-range correlation in DNA sequences has been established [13], the nature and the significance of this correlative property remain under debate [14]. Of previous analysis of interesting scaling behaviors of DNA sequence, the most famous one is the $1/f$-like power law at moderate length scales (typically $10 - 1000$ bp) [10, 15]. Less effort has been performed to examine larger scale correlations, partially due to the lack of very long sequences in the past decades. Recently, large scale structure of DNA sequence, especially complete genomes, has been studied [16]. Such large scale structure at the genomic level contains the global evolution information which is lack in small scale one. Traditional methods, however, is ineffective to analyze long range correlation structure at the whole genome level. For example, local "base-base" correlation is difficult to reveal the corresponding biological meaning [13]; power spectrum analysis is impractical due to computer limitation [16]. The present study gives a different approach which may be applicable to such large scale correlation at the genome level.

We have briefly introduced a hierarchical structure (HS) description of multiple scale structures of DNA sequences [17] based on an earlier HS model for hydrodynamic turbulence [18]. The starting point of the analysis is to construct a nucleotide density fluctuation visualization and the probability density function (PDF) description, then perform a multiple moment scaling analysis [19], and apply the HS scaling model to characterize the fluctuation structure. This methodology makes it possible to study correlation structures up to more than 10^5 bp. Our analysis reveals that the nucleotide composition variations along genomes are far from random, but present a complex self-organized structure, called intermittent structure, which can be captured by the HS analysis. In this work, we will show that a detailed study of the systematic variation of HS parameter β measured from more than one hundred sequences of four kingdoms (Bacteria, Archaea, human chromosomes and

*Electronic address: she@pku.edu.cn

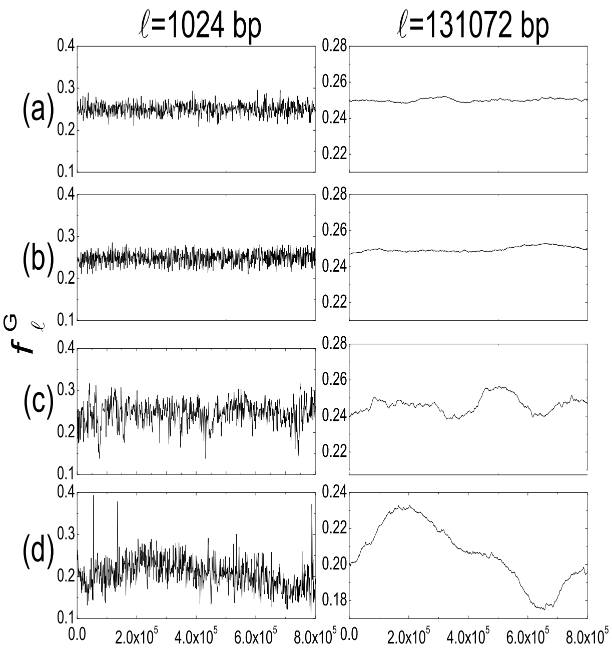

FIG. 1: Nucleotide guanine density (G) variation f^G_ℓ of (a) Random, (b) Simulation, (c) Ecoli and (d) Hsap4. Local densities are calculated over a window of $\ell_{min} = 2^{10}$ bp (the left) and $\ell_{max} = 2^{17}$ bp (the right), respectively. The sliding window moves at a step of length $\Delta = 1024$ bp. Note the intensive fluctuation of natural sequence away from artificial ones.

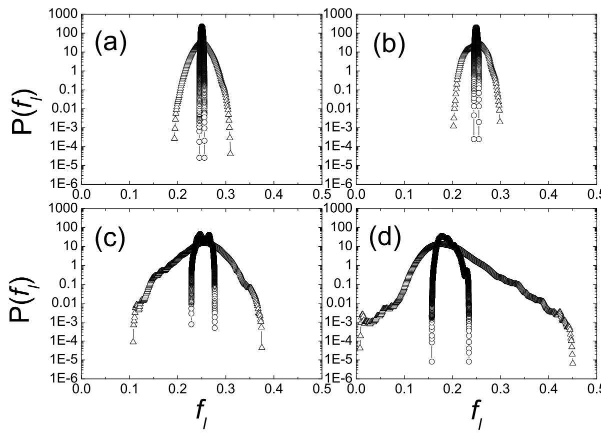

FIG. 2: Typical PDFs of guanine density (G) f_ℓ of (a) Random, (b) Simulation, (c) Ecoli and (d) Hsap4 at two scales $\ell_{min} = 2^{10}$ (circle) and $\ell_{max} = 2^{17}$ (triangle). Note that with ℓ decreasing, the right wings of PDFs progress further, indicating the appearance of high intensity fluctuations in f_ℓ which can be captured by the HS analysis.

viruses) reveals significantly biological information, such as strand symmetry, phylogenetic relations and horizontal gene transfer.

The paper is organized as follows: A multi-scale variable f_ℓ concerning base composition fluctuations of genome sequences is introduced in Sec. II. We present briefly measurements of scaling property with special emphasis on the HS model and similarity test (β-test) in Sec. III. Section IV is devoted to a detailed HS analysis of various kinds of genome data. Section V offers a summary and some additional discussion.

II. BASE COMPOSITION FLUCTUATIONS

A single-stranded DNA chain can be viewed as a symbolic series $\{n_i\}(i = 1, 2, ..., L)$ of length L comprised of four nucleotides A, C, G and T. There are many kinds of transformation of DNA sequences to capturing certain properties, such as the "DNA walk" [9], which construct a numerical sequence $\{u_i\}$ by a certain mapping rule (e.g., adenine rule: if $n_i = A$ then $u_i = 1$; in all other cases $u_i = 0$). Then a running sum $y(n) = \sum_{i=1}^{n}[u_i - (1 - u_i)]$ can be presented graphically as a one-dimensional landscape of the original DNA sequence. Here we employ an alternative approach that introduces a window with length ℓ bp on the DNA sequence, and define the (local) density of a particular base as

$$f_\ell = \frac{1}{\ell}\sum_{k=i}^{i+\ell-1} u_i, \tag{1}$$

where i is the location of the first base within the window. The definition can be used to any single nucleotide (A, C, G, or T) or their degeneracy (R, Y, etc.) and to any dinucleotide molecules (AT, AG, etc.). By sliding the window with a certain moving step Δ and changing the window size ℓ along the DNA sequence, we can obtain different fluctuation sequences f_ℓ. When $\ell = L$, f_ℓ become the mean content of the nucleotide in the entire DNA chain. This multi-scale variable f_ℓ, similar to the locally averaged energy dissipation rate ϵ_ℓ in the turbulence field, is the coarse gaining of base density of the original DNA sequence, which allow us to calculate the probability density functions (PDF) $P(f_\ell)$ and other quantities of f_ℓ of interest.

The fluctuation structures of DNA sequences can be shown by a plot of local base density f_ℓ against the sequence position. Figure 1 displays a segment of 0.8 million bp guanine density (G) fluctuations f_ℓ with two scales 2^{10} ($\approx 10^3$ bp) and 2^{17} ($\approx 10^5$ bp) for four sequences: an independent identical distribution (*i.i.d.*) random sequence with ten million bp and 50% A+T content (Random), a simulated genome sequence with one million bp by the minimal model (Simulation) [20], *E. coli* whole genome (Ecoli) and *H. sapiens* chromosome 4 contig 8 (Hsap4), respectively. The random sequence shows

no surprising white noise signal at both scales and has the least fluctuations amplitude. The simulated sequence contains some visible tips but in a whole is stationary. The *E. coli* genome contains many low guanine density region which is atypical to the main body. The Hsap4 sequence with the special high guanine density seems most intermittent, which include many strong bursts breaking against the background and the highest fluctuation amplitude among the four. We believe that the transition of the fluctuation from small scales to large ones is of special interest to reveal the global information of genome.

With the multi-scale variable f_ℓ, we can carry out the multi-scale PDF method to characterize the interesting structures of such sequences. Firstly we perform an analytical discussion on the random control sequence called *i.i.d.*, i.e., the probability p of each base with $u_i = 1$ (guanine rule) is equal to 0.25. For a certain window size ℓ, the number of guanine in the window $\sum u_i$ exactly obeys the binomial distribution $B(\ell, p)$ [21]. Thus the PDF of the density f_ℓ with a binomial shape is asymmetrical when the of trials is small, and approximates to be symmetrical when the number of trials large enough. Furthermore, if the "success" probability p of each trial is fixed between 0 and 1 (here $p = 0.25$), binomial distribution will approximate to Gaussian distribution. So for the larger window size, PDFs of f_ℓ will have a Gaussian shape. We find that at a small scale (less than several hundred bp) the right wing of f_ℓ extends further more than that of left wing. When scale $\ell \approx 10^3$ bp, the shape of PDFs becomes nearly symmetrical and Gaussian-like (data not shown here) which indicates the vanishing of window size effects. We hereafter analyze natural DNA sequences beyond this scale. Careful calculation of PDFs make it possible to investigate the fluctuation structures at very large scales up to 10^5 bp, about 1/2 to 1/100 of a typical microbial genome. For eukaryotic genome such as the human chromosomes, larger scales are more practical to study. But for comparison, the scale ranges are fixed between 10^3 and 10^5 for all sequences studied below.

The evolution of the PDFs of guanine density fluctuation within the scale range $\ell = 2^{10} \sim 2^{17}$ bp for the full length of the four sequences in Fig. 1 are shown in Fig. 2 where only two scales $\ell_{min} = 2^{10}$ and $\ell_{max} = 2^{17}$ are displayed. With scale ℓ increasing, the distribution of tails progresses further, indicating the emergence of highly intense fluctuations in f_ℓ. The four sets of PDFs show distinct shapes. Both random and simulated sequences have the narrow shapes of PDFs, corresponding to their low fluctuation magnitudes. Moreover, the PDFs of simulated sequence are also symmetrical as those of random sequence. Other two (Ecoli and Hsap4) are not symmetrical. The right wings of the PDFs of Hsap4 are far more higher than the left with an exponential decaying tail, and those of Ecoli is rightly opposite. Such tendencies in the changes of PDFs can be well captured by our quantitative HS analysis below.

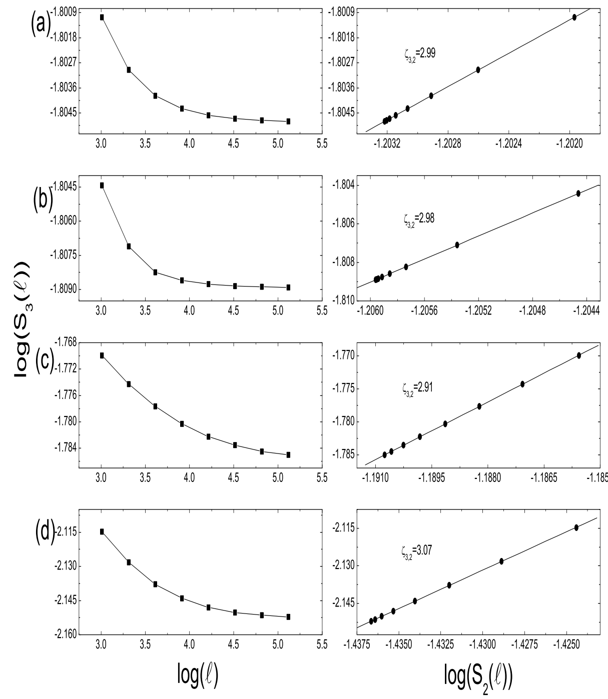

FIG. 3: SS and ESS plots with $S_3(\ell)$ vs. ℓ and $S_3(\ell)$ vs. $S_2(\ell)$ respectively for (a) Random, (b) Simulation, (c) Ecoli and (d) Hsap4. The scale range is $\ell = 2^{10} \sim 2^{17}$. Note the curve of SS plots means no absolute scaling, whereas the linearity of ESS plots means the validation of relative scaling property. The ESS scaling exponents are measured by a least square fitting.

III. MEASUREMENTS

A. Extended self-similarity analysis

Denote by $S_p(\ell)$ the p*th* order moment of the fluctuation f_ℓ:

$$S_p(\ell) = \langle f_\ell^p \rangle = \int f_\ell^p P(f_\ell) df_\ell, \qquad (2)$$

where $P(f_\ell)$ is the PDF of f_ℓ. For the calculation of PDF, we take the linear sequence as a circle, thus all bases in the sequence are treated equally (especially for large ℓ). In fact, most prokaryotic genomes are indeed circular. For large linear eukaryotic chromosomes like those of *H. sapiens* ($L \gg \ell$), the choice of open or close boundary conditions gives essentially the same result.

In previous studies, great efforts were given to explore the power law scaling properties of some quantities like $S_p(\ell)$ with respect to the length sale ℓ: $S_p(\ell) \sim \ell^{\zeta_p}$, called self-similarity (SS), where ζ_p is called the scaling exponents [13]. Consequently, a log-log plot of $S_p(\ell)$ versus ℓ will give a straight line with a slope ζ_p. The DFA method

[22] for analyzing "DNA walk" is such a SS approach. In many cases, however, such abstract scaling property does not hold well. Therefore, a more general scaling relation called extended self-similarity (ESS) [19] has been introduced in turbulence field, which is widely valid even when SS property is not available. The existence of ESS implies that the moments of different orders have a common changing mode with respect to the length scales, thus the ESS is also called relative scaling, with the form like

$$S_p(\ell) \sim S_q(\ell)^{\zeta_{p,q}}, \tag{3}$$

where $\zeta_{p,q}$ is called the relative scaling exponents. log-log plots of $S_3(\ell)$ vs. ℓ for guanine with ℓ ranging from 10^3 to 10^5 bp are shown in Fig. 3(a), where the bended curves indicate the lack of power law scaling for all four sequences. Figure 3 (b) displays plots with $S_3(\ell)$ vs. $S_2(\ell)$, where the perfect linearity verifies the existence of the ESS property in the same scale range. Careful examines for other $S_p(\ell)$ with higher order p (up to order $p = 8$) also show the validation of ESS (data not shown here). The relationship between scaling exponents $\zeta_{p,2}$ with different orders p can be precisely predicted by the HS model as below.

B. Hierarchical structure analysis

The HS model was originally proposed by She and Lévêque [18] to describe inertial-range multi-scale fluctuations in terms of a similarity relation between structures of increasing intensities of successive moment-orders p in the hydrodynamics turbulence fluid. This new similarity relation as a generalization of the Kolmogorov's complete-scale-similarity was later developed as a HS theory [23], which has been successfully applied to analyze many turbulence related field, such as the Couette-Taylor flow [24], flows in rapidly rotating disk [25], the climate turbulence [26], astrophysical magnetohydrodynamic turbulence [27]. and other various complex systems, such as the diffusion-limited aggregates [28], the luminosity fields of natural image [29], chemical reaction patterns [30]. Preliminary analysis of the base density fluctuations at moderate length scales along microbial genomes [31] has given also an encouraging sign that leads to the present work.

The HS model introduces a hierarchy of functions for successive fluctuation intensities:

$$\mu_p(\ell) = \frac{S_{p+1}(\ell)}{S_p(\ell)} = \frac{\int f_\ell^{p+1} P(f_\ell) df_\ell}{\int f_\ell^p P(f_\ell) df_\ell} = \int f_\ell Q_p(f_\ell) df_\ell, \tag{4}$$

where $Q_p(f_\ell) = \frac{f_\ell^p P(f_\ell) df_\ell}{\int f_\ell^p P(f_\ell) df_\ell}$, which is a weighted PDF for which $\mu_p(\ell)$ is the mathematical expectation. Such a hierarchy $\mu_p(\ell)$ covers the mean density fluctuation intensity μ_0, and a series of increasing hierarchical intensities with increasing order p, and finally approaches to the intensity of the so-called most intermittent structure, $\mu_\infty(\ell) = \lim_{p\to\infty} \mu_p(\ell)$. Therefore, one can associate each intensity with an appropriate order p which varies continuously from 0 to infinity. The increasing hierarchical intensity reflects the increasing contribution of positive fluctuation events while reduce that of negative ones. When p is small (less than 10), the hierarchical function μ_p is dominated by the struggle of negative and positive components of bold fluctuations (which is presented by the shape of PDFs).

Note that $\mu_p(\ell)$ is a function of both ℓ and p, which is an inherent merit of the HS model: both scales and intensities are related to describe the multi-scaling property of fluctuation structures. The HS model postulates a relation among various intensities, called HS similarity, with the form like:

$$\frac{\mu_{p+1}(\ell)}{\mu_1(\ell)} = \frac{\alpha_p}{\alpha_0}\left(\frac{\mu_p(\ell)}{\mu_0(\ell)}\right)^\beta, \tag{5}$$

where the exponent β is a constant and α_p is independent of ℓ. The validation of the HS similarity relation Eq. (5) can be tested by a so-called β-test [24, 32], which says that a log-log plot of $\mu_{p+1}(\ell)/\mu_1(\ell)$ vs. $\mu_p(\ell)/\mu_0(\ell)$ (often both items are normalized by the smallest scale ℓ_0) can be constructed, and the HS similarity is satisfied as long as a linearity is observed. Then the HS parameter β can be obtained by measuring the slope using the least square fitting. Technically speaking, this completes the HS analysis of a given set fluctuation data.

The HS theory can construct a scaling equation to predict the ESS scaling exponents. Equation (5) leads to a general formula of the scaling exponents:

$$\zeta_{p,2} = \gamma p + C(1-\beta^p), \tag{6}$$

where $C = (1-2\gamma)/(1-\beta^2)$ is determined by $\zeta_{2,2} = 1$. The parameter γ is introduced to characterize the most intermittent structure: $\mu_\infty(\ell) \sim S_2^\gamma$. Note that $S_0(\ell) \equiv 1$, $S_1(\ell) \equiv C_0$ where C_0 is the average density, and both constants are independent of the scale ℓ and of $S_2(\ell)$, thus we have the exact results $\zeta_{0,2} = 0$, $\zeta_{1,2} = 0$ and $\zeta_{1,2} = 0$. The first constraint is automatically satisfied by Eq. (7), but the second constraint introduces a relation between the parameter β and γ to make only one of them independent. Therefore, the HS model here leaves only one free parameter to describe multi-scaling exponents of the nucleotide density fluctuations. An analysis shows [17]:

$$\zeta_{p,2} = \frac{(1-\beta)p - (1-\beta^p)}{(1-\beta)^2}. \tag{7}$$

where $\beta \neq 1$. Note the situation of $\beta \to 1$ means no intermittency, because γ will approximate to infinite. When $\beta = 1$ the (relative) scaling exponents will be a quadratic form $\zeta_{p,2} = p(p-1)/2$ which can be exactly observed in a completely random DNA sequence.

The HS similarity relation Eq. (5) means that functions $\mu_p(\ell)$ obey a generalized similarity relation over

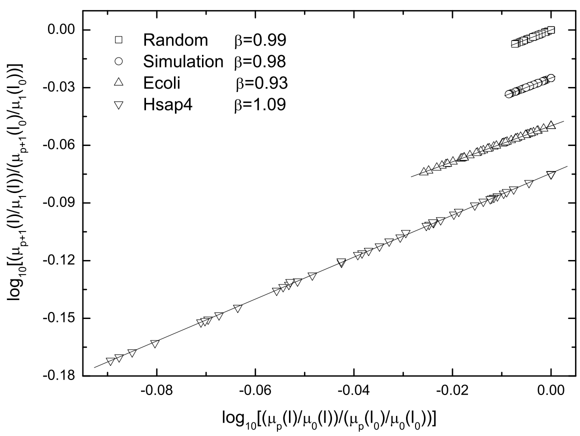

FIG. 4: The β-test of guanine density fluctuation for Random, Simulation, Ecoli and Hsap4 at the range of $2^{10} \leq \ell \leq 2^{17}$ and $0 \leq p \leq 8$. A straight line indicates the validity of the HS similarity. The slope β is estimated by a least square fitting. For clarity, the second, third and fourth set of data points are displaced vertically up by a suitable amount.

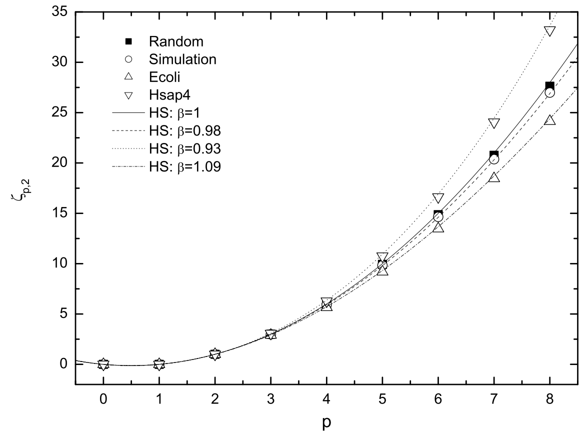

FIG. 5: ESS scaling exponents $\zeta_{p,2}$ of guanine density fluctuation for Random, Simulation, Ecoli and Hsap4. Dotted are the HS model formulas Eq. (7) with β obtained from Fig. 4. Solid lines correspond to a reference $\beta = 1$: $\zeta_{p,2} = p(p-1)/2$. Note that the HS model fits exactly the four sets of scaling exponents.

a range of scales $\ell_1 \leq \ell \leq \ell_2$ and over a range of intensities $p_1 \leq p \leq p_2$. Such a HS similarity is an indication of the self-organization of the ensemble of the fluctuation events. When the HS similarity is presented, the parameter β measures the multi-scale, multi-intensity and self-organized property of the system [23]. When $\beta \to 1$, the system are composed of completely self-similar structures. The corresponding physical picture is the Kolmogorov turbulence, where the large and small-scale statistics are completely self-similar. We will report below if an artificial DNA sequence is completely random, its base density fluctuations will belong to such case. The deviation of β from one means intermittency. Generally speaking, More departure the β, more outstanding the most intermittent structures stand with respect to the background fluctuations. Therefore, the value of β is more intuitively related to the degree of intermittency.

IV. HS ANALYSIS FOR GENOMIC DATA

We conduct the HS analysis for variant kinds of organisms spread all over three kingdoms of species: Eukaryote with *Homo sapiens* (24 chromosomes) and *Saccharomyces cerevisiae cerevisiae* (16 chromosomes); Prokaryote with 16 Archaea complete genomes and 124 Bacteria complete genomes/chromosomes; and 67 viruses complete genomes publicly available in the NCBI RefSeq Release 3, January 30, 2004. For the *H. sapiens* genome, each fully sequenced chromosome composes a few "contigs", which is a draft or finished sequence. Therefore, we select the longest contig (typically large than 10 million bp) in the set of *H. sapiens* chromosomes and analyze them separately. The chromosomes of *S. cerevisiae* are completely sequenced, and thus each was analyzed independently. The 16 Archaea genomes, according to the Bergey's Manual of Systematic Bacteriology (2nd edition), are belong to two phyla: 4 of *Crenarchaeota* and 12 of *Euryarchaeota* [33]. The kingdom of Bacteria is divided into 23 phyla by Bergey's Manual. The 124 species/strains studied here are spread over 13 phyla. Each species/strains is assigned by their 'Bergey Code' for classification as introduced by Qi *et al.* [34]. For example, *Escherichia coli* K12 is listed under Phylum BXII (Proteobacteria), Class III (Gammaproteobacteria), Order XIII (Enterobacteriales), Family I (Enterobacteriaceae), Genus XIII (Escherichia). We change all Roman numerals to Arabic and write the lineage as B.12.3.13.1.13. The 67 viruses sequences studied are long enough (beyond 2^{17} bp) for statistic analysis. Scales for analyzing the nucleotide fluctuations is consistent with the above, from 10^3 to 10^5 bp. For each sequence, four kinds of bases (adenine (A), cytosine (C), guanine (G) and thymine (T)) as four fundamental "words" in DNA sequences are analyzed independently.

Most sequences reasonably pass the β-test (with a correlation coefficient above 0.9995) for four different bases, thus HS parameter β can be obtained from the linear fitting. The measured β of four kinds of bases are listed in Table I $\sim$ Table V, for viruses, Bacteria, Archaea, *S. cerevisiae* and *H. sapiens*, respectively. The β obtained from random sequence and simulated genome sequence with the minimal model is also listed in Table VI to be compared. Some other important information about these

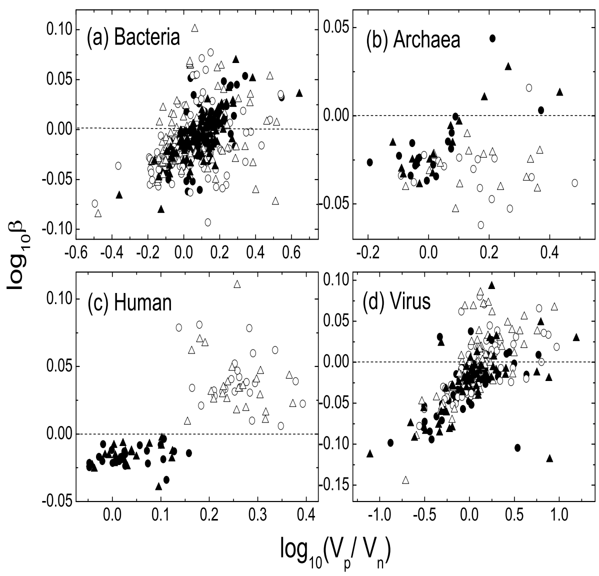

FIG. 6: The log-log plot of β vs. V_p/V_n for (a) Bacteria, (b) Archaea, (c) Human chromosomes and (d) viruses. V_p and V_n is calculated in a window with 1024 bp. Note that β roughly increases with increased amounts V_p/V_n. Where symbols are: (●) A, (▲) T, (○) C, (△), G. Dash lines indicate $\beta = 1$.

sequences, such as names, NCBI accession numbers (Acc. No.), Bergey codes, lengths, base compositions are also listed in the tables. Items are ordered in according to the Bergey code, so species/strains closely related are listed together.

A. The meaning of parameter β

As an example, the results of the β-test for Random, Simulation, Ecoli and Hsap4 are shown in Fig. 4, where the scale range is between 10^3 bp and 10^5 bp and $\ell_0 = 1024$. The exactly good linearity of plots for all four cases indicate that the HS similarity is satisfied, which means that all genomic sequences including the random one have a nicely self-organized HS scaling property. The values of β_G obtained are 0.99 ± 0.000, 0.98 ± 0.000, 0.93 ± 0.001 and 1.09 ± 0.002 for Random, Simulation, Ecoli, and Hsap4, respectively. ESS relative scaling exponents $\zeta_{p,2}$ measured in Fig. 3 as a function of order p are plotted in Fig. 5, where also presents the prediction of HS model Eq. (7) with parameters β obtained in Fig. 4. Good agreements between the data of scaling exponents (points) and HS model predictions (lines) are exactly established. The result of the random sequence analyzed shows that its scaling exponents have a theoretical quadratic form $\zeta_{p,2} = p(p-1)/2$ with β=1. Furthermore, scaling exponents $\zeta_{p,2}$ are distinctly separated into three groups: Random and Simulation with systematically moderate $\zeta_{p,2}$; Hsap4 with larger ones; Ecoli with smaller ones. Theoretical speaking, smaller ESS scaling exponents mean less heterogeneous and high intermittent corresponding to the smaller β. Results of Fig. 5 are consistent well with this theoretical consideration.

The quantitative β values are different for these four sequences. The *i.i.d.* random sequence has a β very close to 1 which is consistent with the self-similarity picture of both its base density fluctuations and the Gaussian-like PDFs. Simulated sequence with β close to 1 indicates that its base density fluctuations are very near to random. Interestingly, Ecoli and Hsap4 have different β values with remarkable deviations from one, where β_G of Ecoli is lower than one and that of Hsap4 is on the opposite. This contrast can also be seen from the opposite fluctuations of the two sequences in Fig. 1. The deviation of β from one is consistent with the increasing of more intermittent structures presented in the guanine density fluctuations shown in Fig. 1 and Fig. 2. The β values measured here give a well quantitative description of this intermittent structures.

Most β values for various genomes in Table I $\sim$ Table V significantly deviate from one, indicating a non-Gaussian statistical property of the base density fluctuations. Mathematically, the existence of β in a range $\ell_1 < \ell < \ell_2$ means that the incremental hierarchical intensity μ_p (p=0,1,...) in this scaling range are linked by a similarity parameter β. μ_p is the mathematical expectation of p order weighted PDF which is directly related to the shape of the original PDF (0-order). If the original PDF is skewed or peaked, the incremental rate of μ_p will deviate from that of a Gaussian PDF, which will lead to the deviation of β from one. Thus β is closely related to the heterogeneity (caused by atypical base density) of the sequence. The measured β, that is dependent on individual organisms, reflects different fluctuation structures of the different genomes.

For illustrating this point, we study the atypical components of the fluctuation signals. When atypical components are biased distribution, e.g., with more positive components than negative ones, the PDF is skewed with a long right tail. V_p is introduced to measure the percentage of the positive components beyond a threshold relative to the whole ensemble:

$$V_p = \int_{\mu+H}^{1} fP(f)df, \tag{8}$$

where f is the base composition measured in a fixed window and μ is the mean value of f. Similarly, the percentage of the negative components V_n is defined as

$$V_n = \int_{0}^{\mu-H} fP(f)df. \tag{9}$$

When calculating V_p and V_n, we fix the window length to be 1024 bp and let H be 1.5 times of standard deviation of f. For reasonable PDF (with a single maximum),

the skewness can be roughly characterized by the relative value of V_p and V_n. When V_p is far more than V_n, the PDF tends to have a long right tail (such as Fig. 2(d)), and vice versa. We study the relationship between β and the biased fluctuation of local base density by a log-log plot β vs. V_p/V_n in Fig. 6 for Bacteria, Archaea, Human chromosomes and viruses respectively. Note that β and V_p/V_n have the same tendency, which relate β with the biased distribution of atypical components. In a word, β measure the heterogeneity of a genome sequence. Although a theory called mutational equilibrium theory [35] for the interpretation of the stationarity of G+C content within a species has been proposed, the understanding (both qualitative and quantitative) on base compositional heterogeneity is still limited. Hereafter we propose β as the "prob" to systematically study the genomic heterogeneity.

The analysis above is focused on the meaning of parameter β in terms of fluctuations of base composition, which is a intuitional study on the physical picture of genome sequences. Such a physical study may have other biological implications. It should be emphasized that HS theory has an mathematical invariance (symmetry) by defining a transformation group [23]. Such a symmetry is exactly achieved through a log-Poisson cascade process [36]. When we carry out multiscaling and hierarchical analysis of DNA, RNA and protein sequences, some transformations or symmetry may be useful to clarify the complexity of a biological system, especially genome data which combine the information of the structure and function together. We think that these quantitative properties, especially HS parameter β, are revelatory to characterize biological questions and farther research should be done. In the following, we will expound two points respectively: DNA strand symmetry in subsec. IV B and sequence complexity with β in subsec. IV C.

B. Strand symmetry

One of the most intriguing results obtained here is that base composition fluctuations of most Prokaryotic genomes and Eukaryotic chromosomes obey a parity rule: $\beta_A \approx \beta_T$ and $\beta_C \approx \beta_G$. This is the extension of Chargaff's parity rule 2 (PR2), which states that if *single strands* of a long DNA duplex (say, a few thousand bp) are isolated and their base compositions are determined, then $\%A \cong \%T$, and $\%C \cong \%G$ [37]. The validity of PR2 became clearer when full genome sequences are calculated. PR2 can be generalized to compositions of dinucleotide and other oligonucleotide [38], or even the whole base-base correlation function [13, 39]. PR2 is generally interpreted as the strand symmetry of biological functionalities such as mutation and/or selection pressures acting on single base or oligonucleotide. Local asymmetrical base composition is also numerously reported [40]. As illustrated in Fig 7 (Top), the local base density of A(G) and T(C) is not equal, but enantiomorphous each other. However, we find the β values of each pair are very close. The parity rule in terms of fluctuation discovered here means that when full genomic sequences are considered, fluctuation structures of A(C) and T(G) are approximately identical, although the local fluctuation at the same position may be different. This point is well illustrated in Fig. 7 (Bottom) in spit of remarkable out-of-phase fluctuations. The existence of PR2 in terms of HS parameter β means that the global function of evolutionary factors, such as mutation pressure or se-

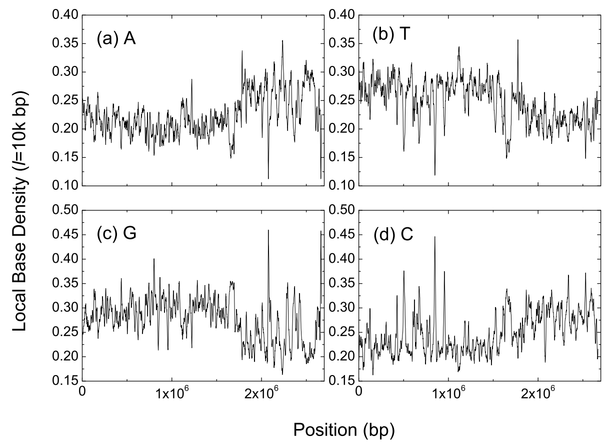

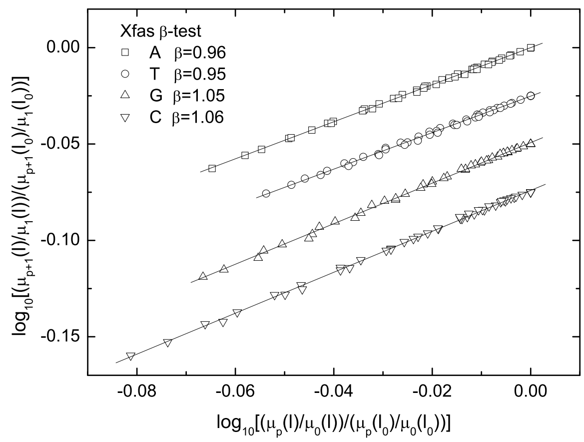

FIG. 7: (Top) Local density fluctuations with a scaling window of $\ell = 10^4$ bp of four bases (a) A, (b) T, (c) G and (d) C for *B-Xfa*. The sliding window moves at a step of length $\Delta = 10^3$ bp. Note the approximately enantiomorphous fluctuation between A and T, G and C; complementary property of base fluctuation between A and G, T and C. (Bottom) β-test of base density fluctuation for *B-Xfa* at the range of $2^{10} \le \ell \le 2^{17}$ and $0 \le p \le 8$. A straight line indicates the validity of the HS similarity. Note that the parity rule $\beta_A \approx \beta_T$ and $\beta_C \approx \beta_G$ is obeyed. For clarity, the second, third and fourth set of data points are displaced vertically up by a suitable amount.

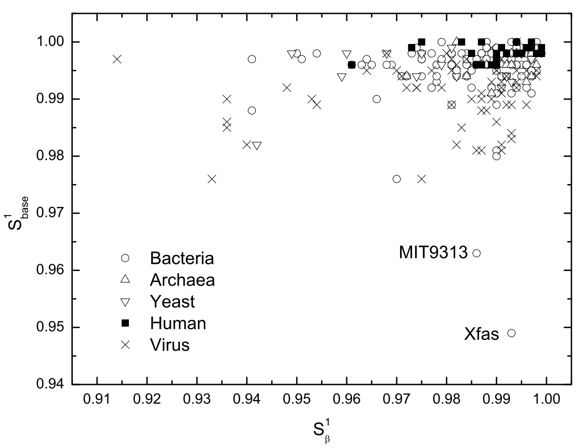

FIG. 8: The symmetry levels S^1_β measured on the base β values of genomes or chromosomes are increased with the increasing sequence length.

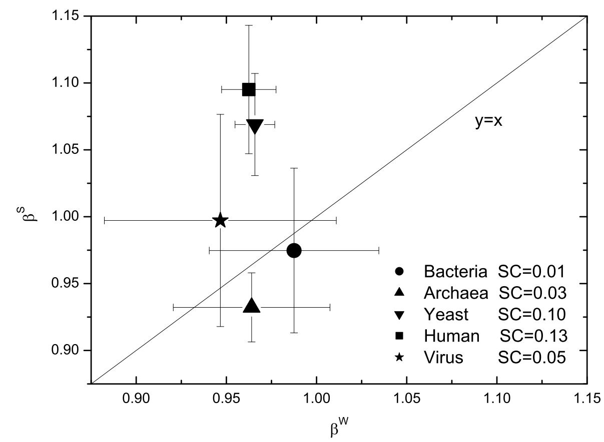

FIG. 9: The mean values of $(\beta_C+\beta_G)/2$ versus $(\beta_A+\beta_T)/2$ for 124 bacterial genomes/chromosomes, 16 archaeal genomes, Yeast, Human and Viruse. The solid points are the mean values Note the cluster property of the three kingdoms and the diversity of viruses.

lection pressure, are not bias on a genomic scale. This finding is consistent with our previous results [17], and such a biological implication may be deserved to study in the future. Recently ref. [41] introduced a similarity function to describe the strand symmetry, which has the form like:

$$S^1 = 1 - \frac{|f_A - f_T| + |f_C - f_G|}{|f_A + f_T| + |f_C + f_G|}, \tag{10}$$

where f_i with $i = \{A, T, C, G\}$ denote the density of any single nucleotide. S^1 can be used to characterize the symmetry level with a range from 0 (asymmetry/dissimilarity) to 1 (prefect symmetry/similarity) (details can be found in Ref. [41]). We calculate S^1_β on the β of four bases, and display the results in Fig. 8, where the symmetry levels roughly increase with the increasing of sequence length.

C. Sequence complexity

Another intriguing results is the systematic change of β with evolutionary categories. The relationship between evolutionary categories and sequences correlation structures have been studied previously in [10, 22, 42]. Note that Buldyrev *et al.* [11] suggested that the complexity of noncoding DNA sequences increased with evolution, with an increasing of spectrum exponents for highly evolved species. While Voss [10] found the spectrum exponents decrease with evolution. These incompatible findings are due to the equivocal meaning of spectrum exponents. We have shown that HS parameter β has an implication of biological evolution [17], that is, the decrease of category averaged β_A reflects the increasing degree of organization in more developed species. As shown in Sec. IV A, we related the decrease of β (of a specific base) with the increasing sequence heterogeneity introduced by concentration of low-density base compositions.

We introduce a new definition of sequence complexity as the total heterogeneity of the four different bases. Because of strand symmetry, we reduce the number of variables from four to two by setting $\beta^S = (\beta_C + \beta_G)/2$ and $\beta^W = (\beta_A+\beta_T)/2$. Then the quantitative expression for sequence complexity is written as:

$$SC = |\beta^S - \beta^W|. \tag{11}$$

For a random sequence, $SC = 0$ because in that case $\beta_A \approx \beta_G$. It establish a zero complexity for random sequences. Complexity of simulated sequence generated by the minimal model [20] is nearly zero. The SC values for different categories, which is shown in Fig. 9, indicate that Human has the highest complexity and Eukaryotes has a higher complexity than Prokaryotes. Interestingly, on average Archaea is more complex than Bacteria. It is not clear if this is because the number of bacterial genomes studied is sufficient to get a statistical average while that of archaeal genomes is biased by its relatively small number of members. But it is remarkable that in this finite set both β^S and β^W of archaea genomes are lower than most of bacteria genomes. This is an interesting phenomenon which needs further study. Virus are very diverse: their β values have a big variance. This may be related to their variability nature.

The relative magnitude of β^S and β^W is also needs further investigation. From Fig. 9 it is clear that for Human $\beta_S > \beta_W$, while Archaea and Bacteria are on the contrary. It indicates the presence of many low-concentration regions of C or G (and hence a high concen-

tration of A or T) in the genomes of prokaryotic genomes. While many regions with high concentration of C or G are spread along the Human genome.

One plausible origin of sequence complexity is horizontal gene transfer (HGT), which has been recognized as one of the major forces in prokaryotic genome evolution [43]. HGT increase the heterogeneity by incorporating alien sequences, because recent transferred sequences from distantly related species have not undergone sufficient mutational pressure, thus its atypical base composition can be distinguished from ancestral DNA [44, 45]. According to this criteria, Garcia-Vallve *et. al.* [45] found that 0% to 22.2% of total genes of 88 bacterial and archaeal genomes are obtained by horizontal gene transfer. The guanine density fluctuation and β-test of three typical cyanobacteria (Thermosynechococcus elongatus BP-1 (BP-1), Synechocystis PCC6803 (PCC6803) and Synechococcus sp. WH8102 (WH8102)) are shown in Fig. 10. WH8102 has a notable small β and extensive low-guanine regions comparing to the other two. Indeed, a lot of low G+C segments of the genome of WH8102 have been comprehensively identified as obtained by HGT [46], contributing to its functionalization of the envelope-modification of the cell surface and the motility of swimming.

V. CONCLUSIONS

Our approach by HS analysis have some merits as the following: first, it has a solid theoretical foundation and has obtained many experimental supports, and varies models deduced from the HS theory has been widely used to analyze nonlinear fields containing intermittent structures; second, It employs an extended scaling analysis which lead to more accurate identification of scaling property; third but not least, the multiple scale fluctuation analysis of base composition is adequate to detect large scale (up to 10^5 bp) correlations.

By carrying out an systematic study of the large scale structures of available genomes, we show that the large scale base density fluctuation ($10^3 - 10^5$ bp) of most examined sequences (including genomes of Archaea, Bacteria, Eukaryotes and viruses) satisfy the HS similarity relation. It reveals that base density fluctuations of genomes are hierarchically organized across scales and across intensities. The HS analysis (β-test) allows one to quantify the degree of multi-scale and multi-intensity correlations. It is known that the major contributing factors to the sequence-wide pattern is not the mean base content and correlations among neighboring bases in genome sequence, but the spatial heterogeneity of the base composition fluctuation or the long-range correlation that largely shapes the complexity of the whole sequence. Our HS parameter β obtained can capture this point. Furthermore, β is effective to describe horizontal gene transfer, strand symmetry, phylogenetic relations of various biological species.

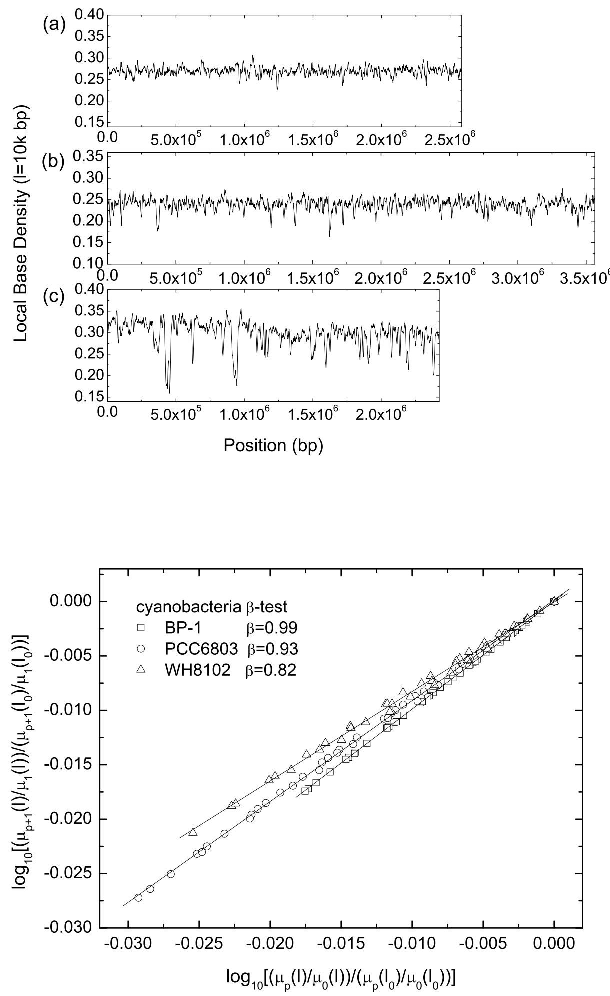

FIG. 10: (Top) Local density fluctuations with a scaling window of $\ell = 10^4$ bp of G for (a) BP-1, (b) PCC6803 and (c) WH8102. The sliding window moves at a step of length $\Delta = 10^3$ bp. (Bottom) β-test for BP-1, PCC6803 and WH8102. The test range is $2^{10} \le \ell \le 2^{17}$ and $0 \le p \le 8$. A straight line indicates the validity of the HS similarity. Note the smaller value of β for WH8102 corresponds to many low-concentration regions of G.

It is shown the values of β for natural DNA sequences show distinct deviation from one which is illustrated as the case of a completely random one. β values show significant divergence, but preserve the parity among bases presumably the consequence of strand symmetry. The HS parameter β are clustered according to evolution categories. It indicate that spatial heterogeneity of base composition or long-range correlation in genomic sequences are different for Archaea, Bacteria and Eukaryotes. The heterogeneity is interpreted as different genetic material transfer patterns for evolutionary communities.

Acknowledgments

We have benefited from useful discussions with many people at the LTCS and CTB of Peking University, especially Dr. Huaiqiu Zhu. This work was supported by NNSFC No. 10225210 and by 973 Project Grant No. 2003CB715905 founded by MOSTof China.

APPENDIX A: ABBREVIATIONS

The abbreviations of the sequence name are alphabetically listed in the parenthesis:

(a) Table I: Virus (Most abbreviations are taken form http://www.ncbi.nlm.nih.gov/ICTVdb): African swine fever virus (*V-AsFV*), Agrotis segetum granulovirus (*V-AsGV*), Amsacta moorei entomopoxvirus (*V-AmEPV*), Autographa californica nucleopolyhedrovirus (*V-AcNPV*), Bovine herpesvirus 1 (*V-BoHV-1*), Bovine herpesvirus 5 (*V-BoHV-5*), Bovine papular stomatitis virus (*V-BPSV*), Callitrichine herpesvirus 3 (*V-CalHV-3*), Camelpox virus (*V-CMLV*), Canarypox virus (*V-CNPV*), Cercopithecine herpesvirus 1 (*V-CeHV-1*), Chimpanzee cytomegalovirus (*V-CCMV*), Choristoneura fumiferana defective nucleopolyhedrovirus (*V-CfDEFNPV*), Cowpox virus (*V-CPXV*), Ectocarpus siliculosus virus (*V-EsV*), Ectromelia virus (*V-ECTV*), Equine herpesvirus 1 (*V-EHV-1*), Equine herpesvirus 2 (*V-EHV-2*), Equine herpesvirus 4 (*V-EHV-4*), Fowlpox virus (*V-FWPV*), Gallid herpesvirus 2 (*V-GaHV-2*), Gallid herpesvirus 3 (*V-GaHV-3*), Goatpox virus (*V-GTPV*), Helicoverpa armigera nucleopolyhedrovirus G4 (*V-HaNPV*), Heliothis zea virus 1 (*V-HzV-1*), Human herpesvirus 1 (*V-HHV-1*), Human herpesvirus 2 (*V-HHV-2*), Human herpesvirus 4 (*V-HHV-4*), Human herpesvirus 5 (*V-HHV-5*), Human herpesvirus 6 (*V-HHV-6*), Human herpesvirus 6B (*V-HHV-6B*), Human herpesvirus 7 (*V-HHV-7*), Human herpesvirus 8 (*V-HHV-8*), Ictalurid herpesvirus 1 (*V-IcHV-1*), Invertebrate iridescent virus 6 (*V-IIV-6*), Lumpy skin disease virus (*V-LSDV*), Lymantria dispar nucleopolyhedrovirus (*V-LdNPV*), Lymphocystis disease virus - isolate China (*V-LCDV*), Macaca mulatta rhadinovirus (*V-MMRV*), Mamestra configurata nucleopolyhedrovirus A (*V-MacoNPV-A*), Mamestra configurata nucleopolyhedrovirus B (*V-MacoNPV-B*), Melanoplus sanguinipes entomopoxvirus (*V-MsEPV*), Meleagrid herpesvirus 1 (*V-MeHV-1*), Molluscum contagiosum virus (*V-MCV*), Monkeypox virus (*V-MPXV*), Mouse cytomegalovirus 1 (*V-MCMV-1*), Myxoma virus (*V-MYXV*), Orf virus (*V-ORFV*), Orgyia pseudotsugata multicapsid nucleopolyhedrovirus (*V-OpMNPV*), Ostreid herpesvirus 1 (*V-OsHV-1*), Paramecium bursaria Chlorella virus 1 (*V-PBCV-1*), Psittacid herpesvirus 1 (*V-PsHV-1*), Rabbit fibroma virus (*V-SFV*), Rabbitpox virus (*V-RPXV*), Rachiplusia ou multiple nucleopolyhedrovirus (*V-RoMNPV*), Rat cytomegalovirus (*V-RCMV*), Sheeppox virus (*V-SPPV*), Shrimp white spot syndrome virus (*V-SWSSV*), Spodoptera exigua nucleopolyhedrovirus (*V-SpeiNPV*), Spodoptera litura nucleopolyhedrovirus (*V-SpltNPV*), Swinepox virus (*V-SWPV*), Tupaia herpesvirus (*V-TuHV*), Vaccinia virus (*V-VACV*), Variola virus (*V-VARV*), Xestia c-nigrum granulovirus (*V-XecnGV*), Yaba monkey tumor virus (*V-YMTV*), Yaba-like disease virus (*V-YLDV*).

(b) Table II: Bacteria: *Agrobacterium tumefaciens* strain C58 C & L (*B-Atu1* & *B-Atu2*), *Aquifex aeolicus* (*B-Aae*), *Bacillus anthracis* A2012 (*B-Ban*), *Bacillus halodurans* (*B-Bha*), *Bacillus subtilis* (*B-Bsu*), *Bacteroides thetaiotaomicron* VPI-5482 (*B-Bth*), *Bifidobacterium longum* NCC2705 (*B-Blo*), *Bordetella bronchiseptica* (*B-Bbr*), *Bordetella parapertussis* (*B-Bpa*), *Bordetella pertussis* (*B-Bpe*), *Borrelia burgdorferi* (*B-Bbu*), *Bradyrhizobium japonicum* (*B-Bja*), *Brucella melitensis* chromosome I & II (*B-Bme1 Brucella suis* chromosome I & II (*B-Bsu1* & *B-Bsu2*), & *B-Bme2*), *Buchnera aphidicola* (*B-Bap*), *Buchnera aphidicola* Sg (*B-BapS*), *Buchnera* sp. APS (*B-Bsp*), *Campylobacter jejuni* (*B-Cje*), *Caulobacter crescentus* (*B-Cre*), *Chlamydia muridarum* (B-*Cmu*), *Chlamydia trachomatis* (*B-Ctr*), *Chlamydophila caviae* GPIC (*B-Cca*), *Chlamydophila pneumoniae* AR39, CWL029, J138 & TW-183 (*B-Cpn1*, *B-Cpn2*, *B-Cpn3* & *B-Cpn4*), *Chlorobium tepidum* TLS (*B-Cte*), *Chromobacterium violaceum* ATCC 12472 (*B-Cvi*), *Clostridium acetobutylicum* ATCC824 (*B-Cac*), *Clostridium perfringens* (*B-Cpe*), *Clostridium tetani* E88 (*B-Cte*), *Corynebacterium efficiens* YS-314 (*B-Cef*), *Corynebacterium glutamicum* (*B-Cgl*), *Coxiella burnetii* (*B-Cbu*), *Deinococcus radiodurans* chromosome 1 & 2 (*B-Dra1* & *B-Dra2*), *Escherichia coli* CFT073, K12, O157:H7 & O157:H7 EDL933 (*B-Eco1*, *B-Eco2*, *B-Eco3* & *B-Eco4*), *Fusobacterium nucleatum* ATCC 25586 (*B-Fnu*), *Haemophilus ducreyi* 35000HP (B-*Hdu*), *Haemophilus influenzae* Rd (*B-Hin*), *Helicobacter hepaticus* (*B-Hhe*), *Helicobacter pylori* 26695 & J99 (*B-Hpy1* & *B-Hpy2*), *Lactobacillus plantarum* (*B-Lpl*), *Lactococcus lactis* sp. IL1403 (*B-Lla*), *Leptospira intrerrogans* I & II (*B-Lin1* & *B-Lin2*), *Listeria innocua* (*B-Lin*), *Listeria monocytogenes* EGD-e (*B-Lmo*), *Mesorhizobium loti* (*B-Mlo*), *Mycobacterium bovis subsp. bovis* AF2122/97 (*B-Mbo*), *Mycobacterium leprae* TN (*B-Mle*), *Mycobacterium tuberculosis* CDC1551 & H37Rv (*B-Mtu1* & *B-Mtu2*), *Mycoplasma gallisepticum* (*B-Mga*), *Mycoplasma genitalium* (*B-Mge*), *Mycoplasma penetrans* (*B-Mpe*), *Mycoplasma pneumoniae* (*B-Mpn*), *Mycoplasma pulmonis* UAB CTIP (*B-Mpu*), *Neisseria meningitidis* MC58 & Z2491 (*B-Nme1* & *B-Nme2*), *Nostoc* sp. PCC7120 (*B-Nsp*), *Oceanobacillus iheyensis* (*B-Oih*), *Pasteurella multocida* PM70 (*B-Pmu*), *Pirellula* sp. (*B-Psp*), *Porphyromonas gingivalis* W83 (*B-Pgi*), *Prochlorococcus marinus* CCMP1375, CCMP1378 & MIT9313 (*B-Pma1*, *B-Pma2* & *B-Pma3*), *Pseudomonas aeruginosa* PA01 (*B-Pae*), *Pseudomonas putida* KT2440 (*B-Ppu*), *Pseudomonas syringae* (*B-Psy*), *Rickettsia conorii* (*B-Rco*), *Rickettsia prowazekii* (*B-Rpr*), *Ralstonia solanacearum* chromosome (*B-Rso*), *Salmonella ty-*

phi (*B-Sty1*), *Salmonella typhimurium* LT2 (*B-Sty2*), *Salmonella typhi* y2 (*B-Sty3*), *Sinorhizobium meliloti* 1021, pSymA & pSymB (*B-Sme1*, *B-Sme2* & *B-Sme3*), *Shewanella oneidensis* MR-1 (*B-Son*), *Shigella flexneri* 2a strain 301 (*B-Sfl*), *Staphylococcus aureus* Mu50, MW2 & N315 (*B-Sau1*, *B-Sau1* & *B-Sau1*), *Staphylococcus epidermidis* ATCC 12228 (*B-Sep*), *Streptococcus agalactiae* 2603 V/R & NEM316 (*B-Sag1* & *B-Sag2*), *Streptococcus mutans* UA159 (*B-Smu*), *Streptococcus pneumoniae* R6 & TIGR4 (*B-Spn1* & *B-Spn2*), *Streptococcus pyogenes* MGAS8232, MGAS315, SF370 & SSI-1 (*B-Spy1*, *B-Spy2*, *B-Spy3* & *B-Spy4*), *Streptomyces coelicolor* A3(2) (*B-Sco*), *Streptomyces avermitilis* MA-4680 (*B-Sav*), *Synechococcus* sp. WH8102 (*B-SspW*), *Synechocystis* sp. PCC6803 (*B-SspP*), *Treponema pallidum* (*B-Tpa*), *Thermoanaerobacter tengcongensis* (*B-Tte*), *Thermosynechococcus elongatus* BP-1 (*B-Tel*), *Thermotoga maritima* (*B-Tma*), *Ureaplasma urealyticum* (*B-Uur*), *Vibrio cholerae* chromosome 1 & 2 (*B-Vch1* & *B-Vch2*), *Vibrio parahaemolyticus* RIMD 2210633 chromosome 1 & 2 (*B-Vpa1* & *B-Vpa2*), *Vibrio vulnificus* CMCP6 chromosome I & II (*B-Vvu1* & *B-Vvu2*), *Wigglesworthia brevipalpis* (*B-Wbr*), *Wolinella succinogenes* (*B-Wsu*), *Xanthomonas axonopodis citri* 306 (*B-Xax*), *Xanthomonas campestris* ATCC 33913 (*B-Xca*), *Xylella fastidiosa* (*B-Xfa*), *Yersinia pestis* strain C092 & KIM (*B-Ype1* & *B-Ype2*).

(c) Table III: Archaea: *Aeropyrum pernix* (*A-Ape*), *Archaeoglobus fulgidus* (*A-Afu*), *Halobacterium* sp. NRC-1 (*A-Hsp*), *Methanobacterium thermoautotrophicum* (*A-Mth*), *Methanococcus jannaschii* (*A-Mja*), *Methanopyrus kandleri* AV19 (*A-Mka*), *Methanosarcina acetivorans* (*A-Mac*), *Methanosarcina mazei* Goe1 (*A-Mma*), *Pyrococcus abyssi* (*A-Pab*), *Pyrococcus furiosus* (*A-Pfu*), *Pyrococcus horikoshii* (*A-Pho*), *Sulfolobus solfataricus* (*A-Sso*), *Sulfolobus tokodaii* (*A-Sto*), *Thermoplasma acidophilum* (*A-Tac*), *Thermoplasma volcanium* (*A-Tvo*).

---

[1] D. Boffelli, M. A. Nobrega and E. M. Rubin, Nature Rev. Genet. **5**, 456 (2004).
[2] N. Banerjee and M. Q. Zhang, Curr. Opin. Microbiol. **5**, 313 (2002).
[3] B. Dujon *et. al.*, Nature, **430**, 35 (2004).
[4] B. V. Reddy and M. W. Pandit, J. Biomol. Struct. Dyn. **12**, 785 (1995).
[5] W. Li, T. Marr, and K. Kaneko, Physica D **75**, 392 (1994).
[6] P. Bernaola-Galván, R. Román-Roldán, and J. L. Oliver, Phys. Rev. E **53**, 5181 (1996).
[7] A. M. Sugden, B. R. Jasny, E. Culotta, and E. Pennisi, Science **300**, 1691 (2003), and related articles in this special issue: Tree of Life.
[8] F. Flam, Science **266**, 1320 (1994); P. Gtaziano, A. Marcella, S. Cecilia, Method Enzymol. **266**, 281 (1996).
[9] C.-K. Peng *et al.*, Nature **356**, 168 (1992).
[10] R. Voss, Phys. Rev. Lett. **68**, 3805 (1992);
[11] S. V. Buldyrev *et al.*, Phys. Rev. E **51**, 5084 (1995).
[12] A. Arneodo, C. Bacry, V. Graves and J. F. Muzy, Phys. Rev. Lett. **74**, 3293 (1995); A. Arneodo *et al.*, Physica A, **249** (1998).
[13] W. Li, Comput. Chem. **21**, 257 (1997).
[14] S. Nee, Nature **357**, 450 (1992); J. Maddox, Nature **358**, 103 (1992); S. Karlin and V. Brendel, Science **259**, 677 (1993).
[15] W. Li and K. Kaneko, Europhys. Lett. **17**, 655 (1992).
[16] M. S. Vieira, Phys. Rev. E **60**, 5932 (1999).
[17] Z. Ouyang, C. Wang and Z.-S. She, Phys. Rev. Lett. (**93**, 078103 (2004).
[18] Z.-S. She and E. Leveque, Phys. Rev. Lett. **72**, 336 (1994).
[19] R. Benzi *et al.*, Phys. Rev. E **48**, 29 (1993).
[20] L.-C. Hsieh, L. Luo, F. Ji, and H. C. Lee, Phys. Rev. Lett. **90**, 018101 (2003).
[21] W. Li, G. Stolovitzky, P. Bernaola-Galván and J. L. Oliver, Genome Res. **8**, 916 (1998).
[22] C.-K. Peng *et al.*, Phys. Rev. E **49**, 1685 (1995).
[23] Z.-S. She, Prog. Theor. Phys. Supp. **130**, 87 (1998).
[24] Z.-S. She, K. Ren, G. S. Lewis and H. L. Swinney, Phys. Rev. E **64**, 016308 (2001).
[25] C. Baroud, B. Plapp, H. Swinney and Z.-S. She, Phys. Fluids **15**, 2091 (2003).
[26] Z.-S. She *et al.*, Prog. in Natural Sci. **12**, 747 (2002).
[27] P. Padoan, S. Boldyrev, W. Langer and A. Nordlund, Astrophys. J. **583**, 308 (2003)
[28] D. Queiros-Conde, Phys. Rev. Lett. **78**, 4426 (1997).
[29] A. Turiel, G. Mato, N. Parga and J.-P. Nadal, Phys. Rev. Lett. **80**, 1098 (1998);
[30] J. Liu *et al.*, Phys. Rev. E **xx**, xxx (2004); J. Liu, Z.-S. She, Q. Ouyang, and X. T. He, Inter. J. Mod. Phys. B **17**, 4139 (2003); H. Y. Guo *et al.*, J. Chem. Phys. **118**, 5038 (2003).
[31] J. Wang, Q. Zhang, K. Ren and Z.-S. She, Chinese Sci. Bull. **46**, 1988 (2001).
[32] Z.-S. She and L. Liu, Acta Mech. Sinica **19**, 453 (2003); L. Liu and Z.-S. She, Fluid Dyn. Res. **33**, 261 (2003).
[33] Bergeys Manual Trust (2nd ed), Springer-Verlag, New York (2001).
[34] J. Qi, B. Wang and B.-L. Hao, J. Mol. Evol. **58**, 1 (2004).
[35] N. Sueoka, Proc. Natl. Acad. Sci. USA **48**, 582 (1962).
[36] B. Dubrulle, Phys. Rev. Lett. **73**, 959 (1994); Z.-S. She and E. C. Waymire, Phys. Rev. Lett. **74**, 262 (1995).
[37] D. R. Forsdyke, Bioinformatics **18**, 215 (2002).
[38] V. V. Prabhu, Nucleic Acids Res. **21**, 2797 (1993).
[39] M. Teitelman and F. H. Eeckman, J. Comput. Biol., **3**, 573 (1996).
[40] J. Mrázek, and S. Karlin, Proc. Natl. Acad. Sci. USA **95**, 3720 (1998).
[41] P. Baisnée, S. Hampson and P. Baldi, Bioinformatics **18**, 1021 (2002).
[42] S. V. Buldyrev *et al.*, Biophys. J. **65**, 2673 (1993); R. Roman-Roldan, P. Bernaola-Galvan and J. L. Oliver, Phys. Rev. Lett. **80**, 1344 (1998).
[43] E. V. Koonin,K. S. Makarova, and L. Aravind, Annu. Rev. Microbiol, **55**, 709 (2001).
[44] J. G. Lawrence and H. Ochman, Proc. Natl. Acad. Sci. USA **95**, 9413 (1998); W. Martin, Bioessays **21**, 99

(1999); A. M. Campbell, Theor. Popul. Biol. **57**, 71 (2000); H. Ochman, J. G. Lawrence and E. A. Groisman, Nature **405**, 299 (2000).

[45] S. Garcia-Vallve, A. Romeu and J. Palau, Genome Res. **10**, 1719 (2000).

[46] B. Palenik *et al.*, Nature **424**, 1037 (2003).

TABLE I: Information of *virus* complete sequences.

Virus	Length	A%	C%	G%	T%	β_A	β_C	β_G	β_T	S^1_{base}	S^1_{beta}	Acc. No.
V-AsFV	170101	0.304	0.194	0.195	0.307	0.926	0.890	0.909	0.964	0.996	0.985	NC_001659
V-AsGV	131680	0.309	0.182	0.191	0.318	0.947	0.938	1.058	1.069	0.982	0.940	NC_005839
V-AmEPV	232392	0.405	0.090	0.088	0.417	0.962	0.970	0.966	0.928	0.986	0.990	NC_002520
V-AcNPV	133894	0.293	0.203	0.204	0.300	0.984	0.952	1.019	0.949	0.992	0.974	NC_001623
V-BoHV-1	135301	0.135	0.359	0.365	0.140	0.899	1.093	1.043	0.925	0.989	0.981	NC_001847
V-BoHV-5	138390	0.124	0.372	0.376	0.128	1.025	1.047	0.964	1.028	0.992	0.979	NC_005261
V-BPSV	134431	0.178	0.322	0.323	0.177	1.029	0.933	0.895	1.118	0.998	0.968	NC_005337
V-CalHV-3	149696	0.262	0.247	0.245	0.245	0.805	1.044	1.025	0.838	0.981	0.986	NC_004367
V-CMLV	205719	0.336	0.166	0.166	0.332	0.941	1.009	0.987	0.962	0.996	0.989	NC_003391
V-CNPV	359853	0.352	0.152	0.152	0.344	0.967	0.984	1.044	0.918	0.992	0.972	NC_005309
V-CeHV-1	156789	0.128	0.369	0.375	0.127	1.074	1.048	1.043	1.055	0.993	0.994	NC_004812
V-CCMV	241087	0.192	0.307	0.310	0.191	0.996	0.886	0.869	0.971	0.996	0.989	NC_003521
V-CfDEFNPV	131158	0.270	0.230	0.229	0.271	1.064	0.964	0.968	0.990	0.998	0.980	NC_005137
V-CPXV	224501	0.333	0.168	0.166	0.333	0.964	1.025	1.000	0.978	0.998	0.990	NC_003663
V-EsV	335593	0.244	0.258	0.260	0.238	0.991	0.999	1.170	0.950	0.992	0.948	NC_002687
V-ECTV	209771	0.335	0.167	0.165	0.334	0.952	1.022	0.977	0.969	0.997	0.984	NC_004105
V-EHV-1	150223	0.217	0.287	0.279	0.216	0.823	1.074	1.094	0.808	0.991	0.991	NC_001491
V-EHV-2	184427	0.216	0.293	0.282	0.209	0.941	0.907	0.875	0.975	0.982	0.982	NC_001650
V-EHV-4	145597	0.249	0.254	0.251	0.247	0.849	1.080	1.090	0.842	0.995	0.996	NC_001844
V-FWPV	288539	0.348	0.154	0.154	0.343	0.928	0.984	1.044	0.959	0.995	0.977	NC_002188
V-GaHV-2	138675	0.283	0.215	0.214	0.287	0.846	1.164	1.165	0.869	0.995	0.994	NC_002229
V-GaHV-3	164270	0.230	0.269	0.267	0.234	0.797	1.086	1.090	0.771	0.994	0.992	NC_002577
V-GTPV	149599	0.380	0.124	0.129	0.367	0.955	0.909	0.941	0.957	0.982	0.991	NC_004003
V-HaNPV	131403	0.301	0.194	0.196	0.309	0.946	0.961	0.978	0.988	0.990	0.985	NC_002654
V-HzV-1	228089	0.288	0.211	0.208	0.293	0.951	0.922	0.905	0.934	0.992	0.991	NC_004156
V-HHV-1	152261	0.159	0.338	0.345	0.158	0.833	1.203	1.181	0.820	0.992	0.991	NC_001806
V-HHV-2	154746	0.149	0.350	0.353	0.147	0.873	1.109	1.076	0.832	0.995	0.981	NC_001798
V-HHV-4	172281	0.198	0.305	0.295	0.203	0.877	0.949	1.117	0.958	0.985	0.936	NC_001345
V-HHV-5	230287	0.216	0.283	0.289	0.212	0.981	0.932	0.889	0.976	0.990	0.987	NC_001347
V-HHV-6	159321	0.289	0.217	0.208	0.287	0.876	0.946	0.924	0.868	0.989	0.992	NC_001664
V-HHV-6B	162114	0.287	0.217	0.211	0.286	0.859	0.955	0.965	0.828	0.993	0.989	NC_000898
V-HHV-7	144861	0.324	0.181	0.172	0.322	0.912	1.001	1.091	0.824	0.989	0.954	NC_001716
V-HHV-8	137508	0.237	0.275	0.260	0.228	1.091	1.021	1.046	1.011	0.976	0.975	NC_003409
V-IcHV-1	134226	0.214	0.281	0.281	0.224	0.887	0.940	1.001	1.075	0.990	0.936	NC_001493
V-IIV-6	212482	0.352	0.148	0.139	0.362	0.960	1.000	0.978	0.933	0.981	0.987	NC_003038
V-LSDV	150773	0.376	0.127	0.132	0.364	0.957	0.915	0.941	0.957	0.983	0.993	NC_003027
V-LdNPV	161046	0.213	0.287	0.288	0.213	0.969	0.919	0.954	0.964	0.999	0.989	NC_001973
V-LCDV	186250	0.363	0.135	0.138	0.365	0.951	1.023	1.136	0.986	0.995	0.964	NC_005902
V-MMRV	133719	0.245	0.267	0.258	0.230	0.896	0.982	1.177	0.971	0.976	0.933	NC_003401
V-MacoNPV-A	155060	0.292	0.207	0.209	0.291	0.958	0.965	0.984	1.015	0.997	0.981	NC_003529
V-MacoNPV-B	158482	0.302	0.199	0.202	0.298	0.978	0.960	0.985	0.988	0.993	0.991	NC_004117
V-MsEPV	236120	0.407	0.092	0.091	0.410	0.980	0.956	0.947	0.945	0.996	0.989	NC_001993
V-MeHV-1	159160	0.260	0.238	0.238	0.265	0.884	1.052	1.049	0.878	0.995	0.998	NC_002641
V-MCV	190289	0.184	0.315	0.318	0.182	1.021	0.929	0.930	0.985	0.995	0.990	NC_001731
V-MPXV	196858	0.335	0.166	0.165	0.334	0.942	1.001	0.996	0.956	0.998	0.995	NC_003310
V-MCMV-1	230278	0.204	0.292	0.295	0.209	1.024	0.939	0.883	0.981	0.992	0.974	NC_004065
V-MYXV	161773	0.287	0.217	0.219	0.278	0.941	1.026	1.018	0.950	0.989	0.996	NC_001132
V-ORFV	139962	0.184	0.318	0.316	0.181	1.021	0.877	0.812	1.069	0.995	0.970	NC_005336
V-OpMNPV	131995	0.223	0.276	0.275	0.225	0.958	0.907	0.976	1.238	0.997	0.914	NC_001875
V-OsHV-1	207439	0.314	0.192	0.195	0.298	0.889	1.033	1.017	0.909	0.981	0.991	NC_005881
V-PBCV-1	330743	0.300	0.201	0.198	0.300	0.967	1.063	1.062	0.931	0.997	0.991	NC_000852
V-PsHV-1	163025	0.193	0.308	0.301	0.198	0.898	1.060	1.070	0.937	0.988	0.988	NC_005264
V-SFV	159857	0.306	0.196	0.199	0.298	0.965	1.035	1.021	0.953	0.989	0.993	NC_001266

TABLE I: (Continued)

Virus	Length	A%	C%	G%	T%	β_A	β_C	β_G	β_T	S^1_{base}	S^1_{beta}	Acc. No.
V-RPXV	197731	0.332	0.168	0.167	0.333	0.952	1.015	1.006	0.974	0.998	0.992	NC_005858
V-RoMNPV	131526	0.302	0.195	0.196	0.307	0.995	0.967	1.036	0.951	0.994	0.971	NC_004323
V-RCMV	230138	0.194	0.301	0.309	0.196	0.786	0.836	0.716	0.761	0.990	0.953	NC_002512
V-SPPV	149955	0.381	0.123	0.127	0.369	0.951	0.917	0.938	0.956	0.984	0.993	NC_004002
V-SWSSV	305107	0.302	0.205	0.205	0.288	0.980	0.972	1.170	0.918	0.986	0.936	NC_003225
V-SpeiNPV	135611	0.283	0.217	0.221	0.278	0.937	1.012	0.991	0.966	0.991	0.987	NC_002169
V-SpltNPV	139342	0.281	0.213	0.215	0.291	0.953	0.906	0.941	0.968	0.988	0.987	NC_003102
V-SWPV	146454	0.366	0.136	0.138	0.360	0.958	0.964	0.985	0.956	0.992	0.994	NC_003389
V-TuHV-1	195859	0.166	0.327	0.340	0.168	0.966	0.901	0.850	0.956	0.985	0.983	NC_002794
V-VACV	191737	0.333	0.167	0.167	0.333	0.986	0.963	0.984	0.984	1.000	0.994	NC_001559
V-VARV	185578	0.338	0.164	0.163	0.334	0.945	1.019	0.998	0.963	0.995	0.990	NC_001611
V-XecnGV	178733	0.297	0.202	0.205	0.296	0.983	0.974	0.935	0.954	0.996	0.982	NC_002331
V-YMTV	134721	0.355	0.148	0.150	0.347	0.941	1.177	1.216	0.949	0.990	0.989	NC_005179
V-YLDV	144575	0.367	0.134	0.136	0.363	0.952	1.153	1.150	0.946	0.994	0.998	NC_002642

TABLE II: Information of Bacteria. The Bergey Code is a shorthand of the lineage of the organism according to the order: phylum, class, order, family, genus. For species/strains (sp/str) belong to the fourteenth phylum, the subclass and suborder is also given. Items are ordered by the Bergey code, so species/strains closely related are listed together.

Beygey code	Sp/str	Length	A%	C%	G%	T%	β_A	β_C	β_G	β_T	S^1_{base}	S^1_{beta}	Acc. No.
B.1.1.1.1.1	*B-Aae*	1551335	0.284	0.217	0.218	0.281	0.888	0.976	0.976	0.901	0.996	0.997	NC_000918
B.2.1.1.1.1	*B-Tma*	1860725	0.270	0.228	0.235	0.268	0.907	0.951	0.928	0.905	0.991	0.993	NC_000853
B.4.1.1.1.1	*B-Dra1*	2648638	0.165	0.335	0.335	0.165	1.118	0.982	0.962	1.053	1.000	0.979	NC_001263
	B-Dra2	412348	0.170	0.333	0.334	0.164	1.132	0.877	0.925	1.173	0.993	0.978	NC_001264
B.10.l	*B-Tel*	2593857	0.231	0.269	0.270	0.230	1.042	0.970	0.993	1.012	0.998	0.987	NC_004113
B.10.1.1.1.11	*B-Pma1*	1751080	0.319	0.182	0.182	0.317	0.971	0.938	1.037	0.978	0.998	0.973	NC_005042
	B-Pma2	1657990	0.345	0.155	0.153	0.347	0.958	0.928	1.062	0.957	0.996	0.965	NC_005072
	B-Pma3	2410873	0.256	0.262	0.245	0.236	0.974	0.884	0.934	0.977	0.963	0.986	NC_005071
B.10.1.1.1.13	*B-SspW*	2434428	0.202	0.297	0.297	0.204	1.077	0.843	0.822	1.085	0.998	0.992	NC_005070
B.10.1.1.1.14	*B-SspP*	3573470	0.261	0.238	0.239	0.262	1.055	0.938	0.927	1.068	0.998	0.994	NC_000911
B.10.1.4.1.8	*B-Nsp*	6413771	0.293	0.206	0.207	0.294	0.985	0.989	1.006	0.975	0.998	0.993	NC_003272
B.11.1.1.1.1	*B-Cte*	2154946	0.219	0.284	0.281	0.216	1.062	0.929	0.923	1.057	0.994	0.997	NC_002932
B.12.1.2.1.1	*B-Rco*	1268755	0.337	0.161	0.163	0.339	0.978	0.995	1.007	0.971	0.996	0.995	NC_003103
	B-Rpr	1111523	0.354	0.144	0.146	0.356	0.955	1.023	1.018	0.988	0.996	0.990	NC_000963
B.12.1.5.1.1	*B-Ccr*	4016947	0.165	0.337	0.335	0.163	0.986	0.994	0.976	1.030	0.996	0.984	NC_002696
B.12.1.6.1.2	*B-Atu1*	2841490	0.205	0.300	0.294	0.202	1.018	0.978	0.977	0.979	0.991	0.990	NC_003304
	B-Atu2	2075560	0.203	0.297	0.296	0.204	1.038	0.959	0.965	1.017	0.998	0.993	NC_003305
B.12.1.6.1.6	*B-Sme1*	3654135	0.186	0.315	0.312	0.186	0.975	0.971	0.971	1.002	0.997	0.993	NC_003047
	B-Sme2	1354226	0.200	0.303	0.301	0.197	0.971	0.992	0.988	0.973	0.995	0.998	NC_003037
	B-Sme3	1683333	0.188	0.311	0.313	0.188	0.991	0.975	0.991	0.974	0.998	0.992	NC_003078
B.12.1.6.3.1	*B-Bme1*	2117144	0.214	0.285	0.287	0.215	1.011	0.963	0.943	1.005	0.997	0.993	NC_003317
	B-Bme2	1177787	0.214	0.286	0.288	0.213	1.006	0.968	0.942	0.970	0.997	0.984	NC_003318
	B-Bsu1	2107792	0.214	0.287	0.285	0.214	1.005	0.946	0.965	1.006	0.998	0.995	NC_004310
	B-Bsu2	1207381	0.213	0.287	0.286	0.214	0.970	0.943	0.970	1.006	0.998	0.984	NC_004311
B.12.1.6.4.6	*B-Mlo*	7036074	0.186	0.316	0.311	0.186	1.000	0.973	0.970	0.992	0.995	0.997	NC_002678
B.12.1.6.7.1	*B-Bja*	9105828	0.180	0.320	0.320	0.180	0.967	0.986	0.980	0.969	1.000	0.998	NC_004463
B.12.2.1.2.1	*B-Rso*	3716413	0.164	0.333	0.337	0.166	1.032	0.946	0.948	1.062	0.994	0.992	NC_003295
B.12.2.1.4.3	*B-Bbr*	5339179	0.159	0.339	0.342	0.160	1.000	0.950	0.978	1.060	0.996	0.978	NC_002927
	B-Bpa	4773551	0.159	0.338	0.343	0.160	1.020	0.952	0.982	1.061	0.994	0.982	NC_002928
	B-Bpe	4086189	0.161	0.337	0.340	0.161	1.011	0.972	0.963	1.013	0.997	0.997	NC_002929
B.12.2.4.1.1	*B-Nme1*	2272351	0.242	0.256	0.260	0.243	0.969	0.917	0.950	0.944	0.995	0.985	NC_003112
	B-Nme2	2184406	0.240	0.259	0.259	0.242	0.970	0.934	0.944	0.962	0.998	0.995	NC_003116
B.12.2.4.1.5	*B-Cvi*	4751080	0.175	0.324	0.324	0.176	1.109	0.881	0.884	1.125	0.999	0.995	NC_005085

TABLE II: (Continued)

Beygey code	Sp/str	Length	A%	C%	G%	T%	β_A	β_C	β_G	β_T	S^1_{base}	S^1_{beta}	Acc. No.
B.12.3.3.1.1	*B-Xax*	5175554	0.176	0.324	0.323	0.176	1.037	0.958	0.951	1.071	0.999	0.990	NC_003919
	B-Xca	5076188	0.175	0.325	0.325	0.174	1.056	0.941	0.958	1.049	0.999	0.994	NC_003902
B.12.3.3.1.9	*B-Xfa*	2679306	0.225	0.249	0.277	0.248	0.962	1.062	1.051	0.946	0.949	0.993	NC_002488
B.12.3.6.2.1	*B-Cbu*	1995275	0.287	0.213	0.213	0.286	1.003	0.967	0.994	0.982	0.999	0.988	NC_002971
B.12.3.9.1.1	*B-Pae*	6264403	0.169	0.336	0.330	0.166	1.107	0.932	0.928	1.100	0.991	0.997	NC_002516
	B-Ppu	6181863	0.192	0.306	0.310	0.193	1.103	0.929	0.925	1.034	0.995	0.982	NC_002947
	B-Psy	6397126	0.208	0.292	0.292	0.208	1.027	0.935	0.928	1.010	1.000	0.994	NC_004578
B.12.3.10.1.7	*B-Son*	4969803	0.270	0.230	0.230	0.270	1.009	0.999	0.969	0.992	1.000	0.988	NC_004347
B.12.3.11.1.1	*B-Vch1*	2961149	0.260	0.238	0.239	0.263	1.040	0.919	0.961	1.033	0.996	0.988	NC_002505
	B-Vch2	1072315	0.265	0.233	0.236	0.266	1.008	0.920	0.956	0.927	0.996	0.969	NC_002506
	B-Vvu1	3281945	0.267	0.231	0.233	0.269	1.042	0.949	0.946	0.970	0.996	0.981	NC_004459
	B-Vvu2	1844853	0.264	0.236	0.235	0.265	0.999	0.935	0.938	1.001	0.998	0.999	NC_004460
	B-Vpa1	3288558	0.272	0.227	0.227	0.274	0.972	0.988	0.974	0.988	0.998	0.992	NC_004603
	B-Vpa2	1877212	0.272	0.227	0.226	0.274	0.983	0.982	0.938	0.979	0.997	0.988	NC_004605
B.12.3.13.1.5	*B-BapS*	641454	0.375	0.125	0.128	0.372	0.942	1.082	1.158	0.984	0.994	0.972	NC_004061
	B-Bsp	640681	0.371	0.131	0.132	0.366	0.954	1.085	1.151	0.978	0.994	0.978	NC_002528
	B-Bap	615980	0.371	0.127	0.127	0.375	0.922	1.016	1.056	0.970	0.996	0.978	NC_004545
B.12.3.13.1.13	*B-Eco1*	5231428	0.248	0.253	0.252	0.247	1.021	0.918	0.923	1.009	0.998	0.996	NC_004431
	B-Eco2	4639221	0.246	0.254	0.254	0.246	1.023	0.925	0.934	1.005	1.000	0.993	NC_000913
	B-Eco3	5498450	0.248	0.252	0.253	0.247	1.028	0.918	0.934	1.025	0.998	0.995	NC_002695
	B-Eco4	5528445	0.248	0.252	0.252	0.247	1.028	0.920	0.927	1.026	0.999	0.998	NC_002655
B.12.3.13.1.32	*B-Sty1*	4809037	0.239	0.260	0.261	0.240	1.014	0.922	0.929	1.010	0.998	0.997	NC_003198
	B-Sty2	4857432	0.239	0.261	0.261	0.239	1.024	0.928	0.925	1.003	1.000	0.994	NC_003197
	B-Sty3	4791961	0.239	0.260	0.261	0.240	1.025	0.912	0.930	1.015	0.998	0.993	NC_004631
B.12.3.13.1.34	*B-Sfl*	4607203	0.246	0.255	0.254	0.245	1.043	0.951	0.931	1.020	0.998	0.989	NC_004337
B.12.3.13.1.38	*B-Wbr*	697724	0.388	0.113	0.112	0.387	0.906	1.044	1.083	0.920	0.998	0.987	NC_004344
B.12.3.13.1.40	*B-Ype1*	4653728	0.262	0.237	0.239	0.262	1.024	0.937	0.944	1.018	0.998	0.997	NC_003143
	B-Ype2	4600755	0.261	0.237	0.239	0.263	1.023	0.952	0.930	1.021	0.996	0.994	NC_004088
B.12.3.14.1.1	*B-Pmu*	2257487	0.299	0.199	0.205	0.297	1.005	0.979	0.997	1.001	0.992	0.994	NC_002663
B.12.3.14.1.3	*B-Hin*	1830138	0.310	0.192	0.190	0.308	0.979	1.045	1.051	0.990	0.996	0.996	NC_000907
	B-Hdu	1698955	0.305	0.185	0.197	0.312	0.980	1.015	1.025	0.949	0.981	0.990	NC_002940
B.12.5.1.1.1	*B-Cje*	1641481	0.348	0.153	0.152	0.346	0.981	0.880	0.960	0.965	0.997	0.975	NC_002163
B.12.5.1.2.1	*B-Hpy1*	1667867	0.303	0.196	0.193	0.308	0.981	0.956	0.950	1.016	0.992	0.989	NC_000915
	B-Hpy2	1643831	0.303	0.197	0.195	0.305	0.983	0.957	0.948	0.996	0.996	0.994	NC_000921
	B-Hhe	1799146	0.322	0.182	0.177	0.319	0.996	0.946	0.931	0.997	0.992	0.996	NC_004917
B.12.5.1.2.2	*B-Wsu*	2110355	0.257	0.239	0.245	0.259	1.083	0.914	0.947	1.026	0.992	0.977	NC_005090
B.13.1.1.1.1	*B-Cac*	3940880	0.346	0.154	0.155	0.345	0.891	0.807	0.965	0.896	0.998	0.954	NC_003030
	B-Cpe	3031430	0.350	0.147	0.138	0.365	0.867	0.913	1.015	0.858	0.976	0.970	NC_003366
	B-Cte	2799251	0.353	0.146	0.141	0.359	0.870	0.952	0.925	0.830	0.989	0.981	NC_004557
B.13.1.2.1.8	*B-Tte*	2689445	0.312	0.188	0.188	0.313	0.938	0.876	0.912	0.930	0.999	0.988	NC_003869
B.13.2.1.1.1	*B-Mge*	580074	0.346	0.158	0.159	0.337	0.978	0.984	1.072	0.930	0.990	0.966	NC_000908
	B-Mpe	1358633	0.370	0.128	0.129	0.372	0.945	1.179	0.948	0.951	0.997	0.941	NC_004432
	B-Mpn	816394	0.305	0.200	0.201	0.295	0.990	1.017	0.998	0.970	0.989	0.990	NC_000912
	B-Mpu	963879	0.370	0.133	0.133	0.364	0.917	1.195	1.261	0.918	0.994	0.984	NC_002771
	B-Mga	996422	0.345	0.157	0.157	0.341	0.959	1.010	1.158	0.950	0.996	0.961	NC_004829
B.13.2.1.1.4	*B-Uur*	751719	0.373	0.126	0.129	0.372	0.954	0.993	1.130	0.944	0.996	0.963	NC_002162
B.13.3.1.1	*B-Oih*	3630528	0.321	0.179	0.178	0.322	0.943	0.924	1.009	0.934	0.998	0.975	NC_004193
B.13.3.1.1.1	*B-Ban*	5093554	0.323	0.178	0.175	0.325	0.939	0.865	0.890	0.951	0.995	0.990	NC_003995
	B-Bha	4202353	0.282	0.217	0.220	0.281	0.966	0.912	0.932	0.971	0.996	0.993	NC_002570
	B-Bsu	4214814	0.282	0.218	0.217	0.283	0.941	0.931	0.957	0.941	0.998	0.993	NC_000964
B.13.3.1.4.1	*B-Lin*	3011208	0.313	0.189	0.186	0.313	0.930	1.061	1.006	0.924	0.997	0.984	NC_003212
	B-Lmo	2944528	0.310	0.191	0.189	0.310	0.942	1.057	1.000	0.933	0.998	0.983	NC_003210
B.13.3.1.5.1	*B-Sau1*	2878040	0.335	0.164	0.165	0.337	0.927	1.069	0.999	0.956	0.997	0.975	NC_002758
	B-Sau2	2820462	0.334	0.164	0.164	0.338	0.924	1.068	1.028	0.959	0.996	0.981	NC_003923
	B-Sau3	2814816	0.334	0.164	0.164	0.337	0.929	1.073	1.003	0.959	0.997	0.975	NC_002745
	B-Sep	2499279	0.335	0.162	0.159	0.344	0.945	1.148	0.934	0.966	0.988	0.941	NC_004461
B.13.3.2.1.1	*B-Lpl*	3308274	0.277	0.223	0.222	0.278	0.986	0.882	0.907	0.980	0.998	0.992	NC_004567
B.13.3.2.6.1	*B-Sag1*	2160267	0.323	0.179	0.178	0.321	0.980	0.920	1.095	0.962	0.997	0.951	NC_004116

TABLE II: (Continued)

Beygey code	Sp/str	Length	A%	C%	G%	T%	β_A	β_C	β_G	β_T	S^1_{base}	S^1_{beta}	Acc. No.
	B-Sag2	2211485	0.323	0.178	0.178	0.321	0.982	0.918	1.103	0.969	0.998	0.950	NC_004368
	B-Smu	2030921	0.315	0.185	0.183	0.317	0.986	1.068	1.028	0.988	0.996	0.990	NC_004350
	B-Spn1	2038615	0.302	0.198	0.199	0.301	0.993	0.905	0.890	0.999	0.998	0.994	NC_003098
	B-Spn2	2160837	0.303	0.198	0.199	0.300	0.995	0.890	1.016	0.995	0.996	0.968	NC_003028
	B-Spy1	1895017	0.307	0.192	0.193	0.308	0.970	0.970	1.036	0.979	0.998	0.981	NC_003485
	B-Spy2	1900521	0.305	0.194	0.192	0.309	0.972	0.971	1.067	0.975	0.994	0.975	NC_004070
	B-Spy3	1852441	0.309	0.191	0.194	0.306	0.977	0.973	1.034	0.976	0.994	0.984	NC_002737
	B-Spy4	1894275	0.309	0.190	0.195	0.306	0.978	0.961	1.014	0.972	0.992	0.985	NC_004606
B.13.3.2.6.2	*B-Lla*	2365589	0.324	0.176	0.178	0.323	0.956	1.090	0.973	0.985	0.997	0.964	NC_002662
B.14.(1.5).(1.7).1.1	*B-Cef*	3147090	0.184	0.315	0.316	0.185	1.038	0.966	0.959	1.040	0.998	0.998	NC_004369
	B-Cgl	3309401	0.231	0.270	0.268	0.231	0.953	0.980	1.003	0.960	0.998	0.992	NC_003450
B.14.(1.5).(1.7).4.1	*B-Mle*	3268203	0.210	0.287	0.291	0.212	0.971	0.959	0.957	1.005	0.994	0.991	NC_002677
	B-Mtu1	4403836	0.172	0.329	0.327	0.172	0.962	1.134	1.159	0.975	0.998	0.991	NC_002755
	B-Mtu2	4411529	0.172	0.329	0.327	0.172	0.964	1.133	1.163	0.974	0.998	0.991	NC_000962
	B-Mbo	4345492	0.172	0.329	0.327	0.172	0.973	1.135	1.169	0.976	0.998	0.991	NC_002945
B.14.(1.5).(1.11).1.1	*B-Sco*	8667507	0.139	0.360	0.361	0.140	1.007	0.987	0.985	1.011	0.998	0.998	NC_003888
	B-Sav	9025608	0.147	0.354	0.353	0.146	1.020	1.034	0.985	1.016	0.998	0.987	NC_003155
B.14.(1.5).2.1.1	*B-Blo*	2256646	0.200	0.301	0.301	0.199	1.126	0.974	0.947	1.045	0.999	0.974	NC_004307
B.15.1.1.1.4	*B-Psp*	7145576	0.224	0.279	0.275	0.222	0.990	0.987	1.016	0.989	0.994	0.992	NC_005027
B.16.1.1.1.1	*B-Cmu*	1072950	0.299	0.201	0.202	0.298	0.976	0.899	0.957	0.990	0.998	0.981	NC_002620
	B-Ctr	1042519	0.294	0.206	0.207	0.293	0.976	0.893	0.959	0.997	0.998	0.977	NC_000117
B.16.1.1.1.2	*B-Cpn1*	1229858	0.296	0.203	0.203	0.299	0.996	1.000	0.955	0.983	0.997	0.985	NC_002179
	B-Cpn2	1230230	0.299	0.203	0.203	0.296	0.983	0.954	1.000	0.996	0.997	0.985	NC_000922
	B-Cpn3	1226565	0.299	0.203	0.203	0.296	0.984	0.954	0.998	0.995	0.997	0.986	NC_002491
	B-Cpn4	1225935	0.304	0.196	0.196	0.303	0.984	0.954	0.999	0.995	0.996	0.986	NC_005043
	B-Cca	1173390	0.299	0.203	0.202	0.296	0.988	0.977	0.985	0.991	0.999	0.997	NC_003361
B.17.1.1.1.2	*B-Bbu*	910724	0.355	0.144	0.142	0.359	0.952	0.964	0.869	0.966	0.994	0.971	NC_001318
B.17.1.1.1.9	*B-Tpa*	1138011	0.235	0.262	0.266	0.237	0.974	0.903	0.898	0.959	0.994	0.995	NC_000919
B.17.1.1.3.2	*B-Lin1*	4332241	0.325	0.174	0.176	0.325	0.963	0.977	0.972	0.959	0.998	0.998	NC_004342
	B-Lin2	358943	0.324	0.175	0.177	0.325	0.998	0.981	0.960	0.938	0.997	0.979	NC_004343
B.20.1.1.1.1	*B-Bth*	6260361	0.285	0.213	0.215	0.287	0.957	0.896	0.900	0.945	0.996	0.996	NC_004663
B.20.1.1.3.1	*B-Pgi*	2343476	0.258	0.241	0.242	0.259	1.010	0.925	0.934	1.012	0.998	0.997	NC_002950
B.21.1.1.1.1	*B-Fnu*	2174500	0.358	0.140	0.132	0.370	0.887	0.873	0.846	0.895	0.980	0.990	NC_003454

TABLE III: Information of Archaea. The Bergey code is the lineage of the organism according to the order: phylum, class, order, family, genus. Items are ordered by the Bergey code, so species/strains closely related are listed together.

Beygey code	Sp/str	Length	A%	C%	G%	T%	β_A	β_C	β_G	β_T	S^1_{base}	S^1_{beta}	Acc. No.
A.1.1.2.1.3	*A-Ape*	1669695	0.216	0.284	0.280	0.221	0.999	0.933	0.914	1.024	0.991	0.989	NC_000854
A.1.1.3.1.1	*A-Sso*	2992245	0.319	0.179	0.179	0.323	0.947	0.923	0.955	0.944	0.996	0.991	NC_002754
	A-Sto	2694756	0.334	0.163	0.165	0.338	0.965	1.037	0.944	0.950	0.994	0.972	NC_003106
A.2.1.1.1.1	*A-Mth*	1751377	0.251	0.247	0.248	0.254	0.958	0.936	0.939	0.986	0.996	0.992	NC_000916
A.2.6.1.1.1	*A-Afu*	2178400	0.258	0.242	0.244	0.256	0.967	0.910	0.885	0.992	0.996	0.987	NC_000917
A.2.3.1.1.1	*A-Hsp*	2014239	0.161	0.340	0.339	0.160	1.007	0.950	0.949	1.030	0.998	0.994	NC_002607
A.2.2.1.1.1	*A-Mja*	1664970	0.344	0.155	0.159	0.341	0.919	0.916	0.909	0.927	0.993	0.996	NC_000909
A.2.7.1.1.1	*A-Mka*	1694969	0.195	0.307	0.304	0.194	1.106	0.943	0.951	1.065	0.996	0.988	NC_003551
A.2.2.3.1.1	*A-Mac*	5751492	0.285	0.214	0.213	0.288	0.937	0.917	0.911	0.940	0.996	0.998	NC_003552
A.2.2.3.1.1	*A-Mma*	4096345	0.293	0.207	0.208	0.292	0.939	0.925	0.930	0.944	0.998	0.997	NC_003901
A.2.5.1.1.3	*A-Pab*	1765118	0.276	0.224	0.223	0.277	0.925	0.886	0.911	0.926	0.998	0.993	NC_000868
	A-Pfu	1908256	0.296	0.204	0.204	0.296	0.924	0.897	0.953	0.914	1.000	0.982	NC_003413
	A-Pho	1738505	0.290	0.212	0.207	0.291	0.938	0.967	0.922	0.933	0.994	0.984	NC_000961
A.2.4.1.1.1	*A-Tac*	1564906	0.272	0.229	0.231	0.268	0.949	0.947	0.954	0.944	0.994	0.997	NC_002578
	A-Tvo	1584804	0.302	0.199	0.200	0.299	0.941	0.946	0.950	0.965	0.996	0.993	NC_002689

TABLE IV: Information of the *Saccharomyces cerevisiae* genome.

Chromosome	Length	A%	C%	G%	T%	β_A	β_C	β_G	β_T	S^1_{base}	S^1_{beta}
chr1	230203	0.303	0.194	0.199	0.304	0.957	1.072	1.034	0.924	0.994	0.982
chr2	813139	0.307	0.194	0.190	0.310	0.975	1.046	1.054	0.956	0.993	0.993
chr3	316613	0.312	0.197	0.188	0.303	0.942	1.248	1.025	0.960	0.982	0.942
chr4	1531929	0.311	0.189	0.190	0.310	0.994	1.129	1.070	0.951	0.998	0.975
chr5	576869	0.306	0.190	0.195	0.309	0.941	1.024	1.030	0.969	0.992	0.991
chr6	270148	0.307	0.193	0.194	0.306	0.948	1.128	0.980	1.007	0.998	0.949
chr7	1090937	0.310	0.190	0.190	0.309	0.955	1.013	1.011	0.962	0.999	0.998
chr8	562639	0.309	0.194	0.191	0.306	0.990	1.024	1.162	0.959	0.994	0.959
chr9	439885	0.305	0.194	0.195	0.306	0.973	1.006	1.161	0.984	0.998	0.960
chr10	745444	0.310	0.191	0.193	0.306	0.971	1.024	1.128	0.974	0.994	0.974
chr11	666445	0.309	0.192	0.189	0.310	0.972	1.030	1.113	0.968	0.996	0.979
chr12	1078173	0.307	0.193	0.192	0.309	0.966	1.090	1.099	0.971	0.997	0.997
chr13	924430	0.310	0.191	0.191	0.308	0.963	1.050	1.044	0.948	0.998	0.995
chr14	784328	0.308	0.193	0.193	0.306	0.984	1.072	1.200	0.975	0.998	0.968
chr15	1091284	0.311	0.192	0.190	0.307	0.972	1.074	1.054	0.958	0.994	0.992
chr16	948061	0.310	0.190	0.190	0.309	0.950	1.025	0.986	0.987	0.999	0.981

TABLE V: Information of the *Homo sapiens* genome. Contigs used for analysis is list in the column of "contig" and their length is also listed.

Chromosome	Contig	Length	A%	C%	G%	T%	β_A	β_C	β_G	β_T	S^1_{base}	S^1_{beta}
chr1	30	36790572	0.293	0.207	0.207	0.293	0.972	1.148	1.080	0.971	1.000	0.983
chr2	5	84213153	0.306	0.193	0.194	0.307	0.962	1.073	1.080	0.965	0.998	0.998
chr3	2	100530261	0.305	0.195	0.195	0.305	0.962	1.198	1.097	0.959	1.000	0.975
chr4	8	62915881	0.314	0.185	0.186	0.315	0.945	1.098	1.070	0.942	0.998	0.992
chr5	8	41199371	0.307	0.193	0.192	0.307	0.947	1.023	1.037	0.946	0.999	0.996
chr6	6	61695806	0.308	0.192	0.191	0.309	0.966	1.080	1.083	0.964	0.998	0.999
chr7	5	64412912	0.304	0.196	0.196	0.304	0.952	1.094	1.104	0.950	1.000	0.997
chr8	2	48689376	0.306	0.194	0.194	0.305	0.969	1.082	1.074	0.972	0.999	0.997
chr9	1	39435726	0.306	0.195	0.194	0.305	0.952	1.102	1.045	0.956	0.998	0.985
chr10	9	43027086	0.292	0.207	0.207	0.294	0.982	1.077	1.092	0.971	0.998	0.994
chr11	2	48854501	0.296	0.204	0.204	0.297	0.954	1.053	1.052	0.957	0.999	0.999
chr12	8	38627316	0.301	0.200	0.200	0.300	0.955	1.014	1.024	0.948	0.999	0.996
chr13	3	67740325	0.310	0.191	0.190	0.309	0.955	1.083	1.119	0.951	0.998	0.990
chr14	1	87191216	0.294	0.204	0.205	0.297	0.955	1.154	1.113	0.956	0.996	0.990
chr15	2	22003156	0.291	0.211	0.210	0.288	0.958	1.114	1.085	0.983	0.996	0.987
chr16	1	53619965	0.289	0.211	0.211	0.289	0.983	1.091	1.068	0.981	1.000	0.994
chr17	5	24793602	0.282	0.218	0.218	0.283	0.951	1.075	1.175	0.962	0.999	0.973
chr18	3	33548238	0.303	0.197	0.197	0.302	0.981	1.075	1.041	0.984	0.999	0.991
chr19	1	31383029	0.262	0.237	0.238	0.263	0.971	1.067	1.060	0.959	0.998	0.995
chr20	3	26259569	0.289	0.209	0.209	0.293	0.992	1.093	1.061	0.980	0.996	0.989
chr21	1	28602116	0.306	0.196	0.195	0.303	0.971	1.128	1.289	0.964	0.996	0.961
chr22	3	23178213	0.263	0.237	0.237	0.263	0.968	1.050	1.021	0.993	1.000	0.987
chrX	9	32736268	0.304	0.195	0.195	0.307	0.973	1.205	1.167	0.969	0.997	0.990
chrY	1	9938763	0.304	0.194	0.197	0.305	0.925	1.199	1.152	0.913	0.996	0.986

TABLE VI: Information of random and simulated by the minimal model genome.

Chromosome	Length	A%	C%	G%	T%	β_A	β_C	β_G	β_T	S^1_{base}	S^1_{beta}
Random	10000000	0.250	0.250	0.250	0.250	0.994	0.992	0.993	0.992	1.000	0.999
Simulation	1028001	0.270	0.242	0.249	0.239	1.004	0.986	0.979	0.988	0.962	0.994